Am J Transl Res 2020;12(11):7510-7527
www.ajtr.org /ISSN:1943-8141/AJTR0120026

Original Article

Characterization of hazard infiltrating immune cells and relative risk genes in bladder urothelial carcinoma

Yinxiang Lv[1*], Peng Jin[3*], Zheng Chen[2], Peng Zhang[2]

[1]Department of Oncology, People's Hospital of Xinchang County, Xinchang, Zhejiang Province, China; [2]Organ Transplant Center, The Second Affiliated Hospital of Guangzhou Medical University, Guangzhou, Guangdong Province, China; [3]Organ Transplant Center, Xiangya Hospital, Central South University, Changsha, Hunan Province, China. [*]Equal contributors and co-first authors.

Received August 10, 2020; Accepted October 8, 2020; Epub November 15, 2020; Published November 30, 2020

Abstract: Objectives: Bladder urothelial carcinoma (BLCA) is one of the most common malignancies in urinary system. With the development of next-generation sequencing technology, we intended to investigate prognostic immune cells and related signature to predict the prognosis of BLCA and potential therapeutic targets. Methods: We obtained the transcriptome profiles of 573 BLCA patients from The Cancer Genome Atlas (TCGA) and Gene Expression Omnibus (GEO) databases. The fractions of immune cells in each sample was calculated by "CIBERSORT" algorithm. Tumor Infiltrating Immune Cells Scores (TIICS) was accordingly derived and Receiver Operating Characteristic (ROC) curve was conducted to evaluate the predictive efficiency. Moreover, differential analysis was performed between two TIICS groups and hub TIICS-related immune signature was identified. The correlation of key immune genes and immune-infiltrating immune cells was evaluated based on the TIMER database. An Immune Signature Prognostic Index (ISPI) based on these signatures was constructed with superior predictive accuracy. Last, the TIICS model or related immune signature were all validated in an independent cohort from the GSE13507. Results: The least absolute shrinkage and selection operator (LASSO) algorithm was utilized to screen the 6 hub tumor-infiltrating immune cells in TCGA cohort, where higher infiltrating levels of M0 Macrophages, M2 Macrophages and Neutrophils were hazard factors, while $CD8^+$ T cells and memory activated $CD4^+$ T cells were protective factors. Conclusion: Taken together, our study identified several prognostic immune cells and related immune signature in BLCA, shedding insight on the individualized immunotherapy or potential drug targets.

Keywords: Tumor-infiltrating immune cells, immune signature, prognosis, bladder urothelial carcinoma

Introduction

Bladder urothelial carcinoma (BLCA) remains one of the most common malignancies in urinary system and ranks the ninth among all tumors worldwide [1]. Urothelial carcinoma is the main pathological type of bladder cancer, accounting for 90% of all BLCA patients [2, 3]. Since the public awareness of early-detection or development of management, the morbidity of BLCA and tumor-related mortality have increased yearly with the estimated new cases reaching up to 80470 in the United states in 2019 [4]. Though most of bladder cancers do not invade the muscle wall of bladder, nearly 25% of patients inevitably progress into muscle-invasive bladder cancer (MIBC), associated with much worse prognosis [5, 6]. Patients with non-muscle invasive urothelial carcinoma were often treated with transurethral resection of bladder tumor (TURBT) followed by intravesical instillation of Bacillus Calmette-Guerin (BCG) to prevent recurrence [7, 8]. For muscle invasive cases, neoadjuvant chemotherapy using a cisplatin combination regimen plus with radical cystectomy are preferred and the chemotherapy may be chosen as the mainstream treatment for patients with advanced metastasis [9, 10]. However, the efficacy of surgical intervention is limited, and chemotherapy is shown to have multiple side effects, especially the obvious toxicity.

Based on the rapid progression of cancer immune-related therapies during these years, inhibitors of targeted sites in the immune pathway such as programmed death 1 (PD-1) antibody or cytotoxic T-lymphocyte-associated

antigen 4 (CTLA-4) antibody has brought about a major breakthrough in the treatment of locally advanced and metastatic bladder cancer [11, 12]. Currently, multi-centers with large samples of clinical trials have proved the exact efficacy of PD-1/PDL-1 antibody. The American Society of Clinical Oncology (ASCO) in 2017 has declared the superior clinical outcome of pembrolizumab and recommended it as the first-line in treating locally advanced or stage IV metastatic cases to replace traditional cis-platinum regimen, which was released as the guideline by The National Comprehensive Cancer Network (NCCN) in 2018 [13, 14]. Besides, other investigators found that some urinary cytokines may provide additional value to predict responses to immune drugs in patients with NMIBC which shed lights on the importance of feasible immune biomarkers [12, 15, 16]. However, there existed a proportion of BLCA patients revealed limited responses to immunotherapy, indicating the potential heterogeneity in immune treatment across patients. Clinical markers currently used to predict the responsive efficacy of immunotherapy included the expression level of PD-1/PD-L1, luminal or basal subtypes, tumor mutation burden or ECOG scores [17, 18]. However, it is difficult to implement, and the feasibility is limited [19, 20]. Therefore, it is significant to identify robust genes that possessing predictive values for BLCA patients and even served as potential targets for immune therapy.

CIBERSORT was utilized to estimate the proportions of 22 immune cell subtypes using gene expression profiling, which was used in various tumor samples. In our research, we combined the transcriptome data and corresponding clinical information of patients from TCGA-BLCA cohort and GEO databases to construct and confirm a Tumor Infiltrating Immune Cells Scores (TIICS) model consisted of 6 prognostic tumor immune cells. We systematically assessed the prognostic value of TIICS and the relationships with independent clinical characteristics. Besides, we also investigated and identified the potential TIICS-related immune signature associated with immune infiltrates and survival outcomes. Hence, our analysis aimed to provide a comprehensive landscape of prognostic immune infiltration cells with risk immune signature for prediction and offered a foundation in subsequent individualized treatment of BLCA patients.

Methods and materials

Data acquisition and processing

Transcriptome profiling raw data with corresponding clinical information were downloaded from TCGA (https://cancergenome.nih.gov/) and the GEO (https://www.ncbi.nlm.nih.gov/geo/) databases. From TCGA, we obtained 408 BLCA and 25 normal tissues using the GDC tool, in which the mRNA-seq data were processed as the FPKM values. We normalized the RNA expression profiles, and the differential genes analysis was performed by the "edgeR" package. Besides, GSE13507 series consisted of 188 BLCA matched with 68 normal tissues, and we downloaded the series matrix files to conduct normalization of raw data using the "limma" package. In addition, the immune related genes were downloaded and summarized from the Immunology Database and Analysis Portal (ImmPort), which updating and sharing data on immunology research timely. These genes were identified and chosen to further investigate the underlying relationships with tumor immune infiltrates.

Estimated abundance of immune cells and prognostic analysis

CIBERSORT is an advanced method to infer the specific abundances of immune cells based on expression data. We obtained the "CIBERSORT" R script (https://cibersort.stanford.edu/) and conducted the deconvolution algorithm based on the transcriptome data of 408 BLCA samples. The algorithm estimated the fraction of 22 tumor infiltrating immune cells in BLCA. The results were shown in a matrix and the sum of all immune cells equaled 100% in each sample. Meanwhile, univariate Cox regression model and Least Absolute Shrinkage and Selection Operator (LASSO) method were conducted by "survival" and "rms" packages to identify hub prognostic immune cells in BLCA. Multivariate Cox model was used to calculate the coefficients (β_i) of each prognostic immune cells. Then, Tumor Infiltrating Immune Cells Scores (TIICS) was established as: $TIICS = \Sigma (\beta_i * Fraction_i)$. Furthermore, Receiver Operating Characteristic (ROC) curve were used to confirm the predictive significance of prognostic cells and survival analysis was conducted to compare the differential prognosis in patients in two TIICS

levels. The distribution of 22 immune cells were shown in heatmap plot via "heatmap" package and the correlation among cells were calculated by "corrplot" package. In addition, Wilcox rank-sum test was conducted to confirm the various infiltrations of cells in two TIICS levels quantitatively. The survival plots of immune cells were drawn by "survival" package.

Correlation analysis

We extracted several independent risk clinical features from included patients, including tumor grades and TNM stages. The Wilcox rank-sum test was selected only to compare the distributions of TIICSs in two groups, while Kruskal-Wallis (K-W) test was used in three or more groups. We regarded that $P<0.05$ was statistically significant.

Differential analysis, functional pathways, and gene set enrichment analysis (GSEA)

Differentially expressed genes analysis was conducted to identify TIICS related signature between two groups by "limma" packages. The |log (Fold Change)| >1 and false discovery rate (FDR) <0.05 as set as the threshold. Then, we searched the differential immune signature and univariate Cox analysis was utilized to select significantly prognostic ones. The intersect genes were visualized via "Venn Diagram" package. Moreover, the Gene Ontology (GO) and Kyoto Encyclopedia of Genes and Genomes (KEGG) analysis for differential signature were shown in dot plot with various packages consisted of "org.Hs.eg.db", "cluster Profiler", "enrich plot" and "ggplot2" packages. Last, GSEA was performed between high- and low TIICS phenotypes (http://software.broadinstitute.org/gsea/index.jsp) to analyze the immune-related pathways between two groups. We downloaded the "c2.cp.kegg.v6.2.symbols.gmt gene sets" from the MSigDB (http://software.broadinstitute.org/gsea/downloads.jsp) as the reference gene sets. In addition, the enriched gene sets were considered to be significant when FDR was less than 0.25 and the *P* value was less than 0.05.

TIMER database

TIMER (https://cistrome.shinyapps.io/timer/) is a comprehensive immunological resource including more than 10,000 samples across various cancer types from TCGA, mainly focusing on the analysis of tumor immune infiltrates. The abundances of six infiltrated immune cells could be estimated by the database, which is confirmed in well accordance with flow cytometry results. Hence, we further analyzed the relationships between expression of the prognostic immune related genes (IRGs) with the infiltrating abundance of six hub immune cells. The Spearman's correlation coefficient and the estimated statistical significance were calculated. The gene expression level was represented with $\log_2$ RSEM at the y axis. Furthermore, we assessed the mutants of key immune genes with immune infiltrations in BLCA based on the on the "SCNA" module (https://cistrome.shinyapps.io/timer/). The differential infiltrating levels was compared using Wilcox rank-sum test.

Construction of ISPI in BLCA

Since we identified 16 hub immune infiltrating related signature, we constructed an ISPI to predict survival outcomes in BLCA as following: $ISPI = \Sigma (\beta_i * EXP_i)$. Then, we classified the cohorts into two groups with low- and high ISPI. We utilized the ROC to evaluate the predictive significance of ISPI and Kaplan-Meier analysis was used to confirm the prognosis difference between two groups. Meanwhile, The ISPI model was further validated in GSE13507.

Statistical analysis

LASSO regression analysis, Cox regression model or Kaplan-Meier analysis were conducted by "glmnet" and "survival" packages. The Student's t test was used to compare the clinical variables, and Chi-square test was suitable for categorical variables. Wilcoxon rank-sum test was used for comparisons between two groups. The Pearson coefficients were used to determine the correlation between two variables. All statistical analysis was conducted in R studio (version 3.5.3), and the $P<0.05$ was regarded to be significant.

Results

Identification of prognostic tumor immune infiltrating cells in BLCA

The clinical baseline characteristics of included BLCA cohorts were shown in **Table 1**. We calculated the fractions of 22 tumor infiltrating

Table 1. Clinical baseline of all 577 BLCA patients from TCGA cohort and GSE13507

Variables	Training group (n=412)	Validation group (n=165)	Entire group (n=577)
Status			
Alive			
Dead	156 (38.5)	69 (41.8)	225 (43.3)
Age	68±10.57	65.18±11.97	67.19±11.06
Gender			
Female	106 (26.2)	30 (18.2)	136 (23.9)
Male	299 (73.8)	135 (81.8)	434 (76.1)
Race			
White	334 (82.5)	NA	NA
Asian	43 (10.6)	NA	NA
Black or African	28 (6.9)	NA	NA
AJCC-T			
T0/Ta	1 (0.2)	24 (14.5)	25 (4.4)
T1	3 (0.8)	80 (48.5)	83 (14.6)
T2	117 (28.9)	31 (18.8)	148 (25.9)
T3	193 (47.7)	9 (5.5)	212 (37.2)
T4	58 (14.3)	11 (6.7)	69 (12.1)
unknown	33 (8.1)	0 (0.0)	33 (5.8)
AJCC-N			
N0	235 (58.0)	149 (90.3)	384 (67.4)
N1	46 (11.4)	8 (4.9)	54 (9.5)
N2	75 (18.5)	6 (3.6)	81 (14.2)
N3	7 (1.7)	1 (0.6)	8 (1.4)
unknown	42 (10.4)	1 (0.6)	43 (7.5)
AJCC-M			
M0	195 (48.1)	158 (95.8)	353 (61.9)
M1	11 (2.7)	7 (4.2)	18 (3.2)
Mx	199 (49.2)	NA	NA
Pathologic stage			
I & II	130 (32.1)	NA	NA
III & IV	273 (67.4)	NA	NA
unknown	2 (0.5)	NA	NA
Tumor grade			
G1/G2	20 (5.0)	105 (63.6)	125 (21.9)
G3/G4	382 (94.3)	60 (36.4)	442 (77.6)
unknown	3 (0.7)	NA	NA
TIICS level			
Low	203 (50.1)	82 (50.0)	285 (50.0)
High	202 (49.9)	83 (50.0)	285 (50.0)

immune cells in 408 BLCA samples using the gene transcriptome data (**Figure 1A**; Table S1). Then, the LASSO regression analysis screened 6 survival-related immune cells, including M0 Macrophages, M2 Macrophages, $CD8^+$ T cells, memory activated $CD4^+$ T cells, resting Dendritic cells and activated Dendritic cells (**Figure 1B**, **1C**). Univariate Cox analysis revealed that higher infiltrating M0 Macrophages (HR=5.042, P=0.001), M2 Macrophages (HR=4.643, P=0.043) and Neutrophils (HR=3.902, P=0.01) were hazard factors, while $CD8^+$ T cells (HR=0.093, P=0.004) and memory activated $CD4^+$ T cells (HR=0.075, P=0.060) were protective factors (**Table 2**; **Figure 1D**). Though no significant difference of infiltrating levels of Dendritic cells in univariate Cox analysis, the subsequent Kaplan-Meier analysis suggested that lower infiltrating level of Dendritic cells predicted poor survival outcomes (P=0.018). We finally integrated 6 immune cells into the final model consisted of M0 Macrophages, M2 Macrophages, $CD8^+$ T cells, memory activated $CD4^+$ T cells, resting Dendritic cells and activated Dendritic cells. TIICS was calculated by multivariate Cox results and divided the 408 patients into high- and low-TIICS groups (Table S2). Area Under Curve (AUC) of the ROC plot was 0.653, and patients with higher TIICS level revealed poor survival outcomes in Kaplan-Meier curve (P=1e-05, **Figure 1E**, **1F**). To further investigate the differential levels of immune cells in two groups, the heatmap illustrated that M0 Macrophages, M2 Macrophages showed advanced infiltration in high-TIICS group, while memory activated $CD4^+$ T cells, $CD8^+$ T cells were lower infiltrating in low-TIICS group (**Figure 2A**). In addition, the correlation heatmap indicated the coincident and exclusive relationships among immune cells in **Figure 2B**, in which green represented the co-occurrence and red represented the mutually exclusive associations.

The subsequent results of Wilcox rank-sum test and Kaplan-Meier analysis were in line with the previous analysis, in which M0 Macrophages showed higher infiltration in high-TIICS group suggesting poor outcomes, but higher infiltrating level of memory activated $CD4^+$ T cells, $CD8^+$ T cells were protective factors (**Figure 2C**, **2D**).

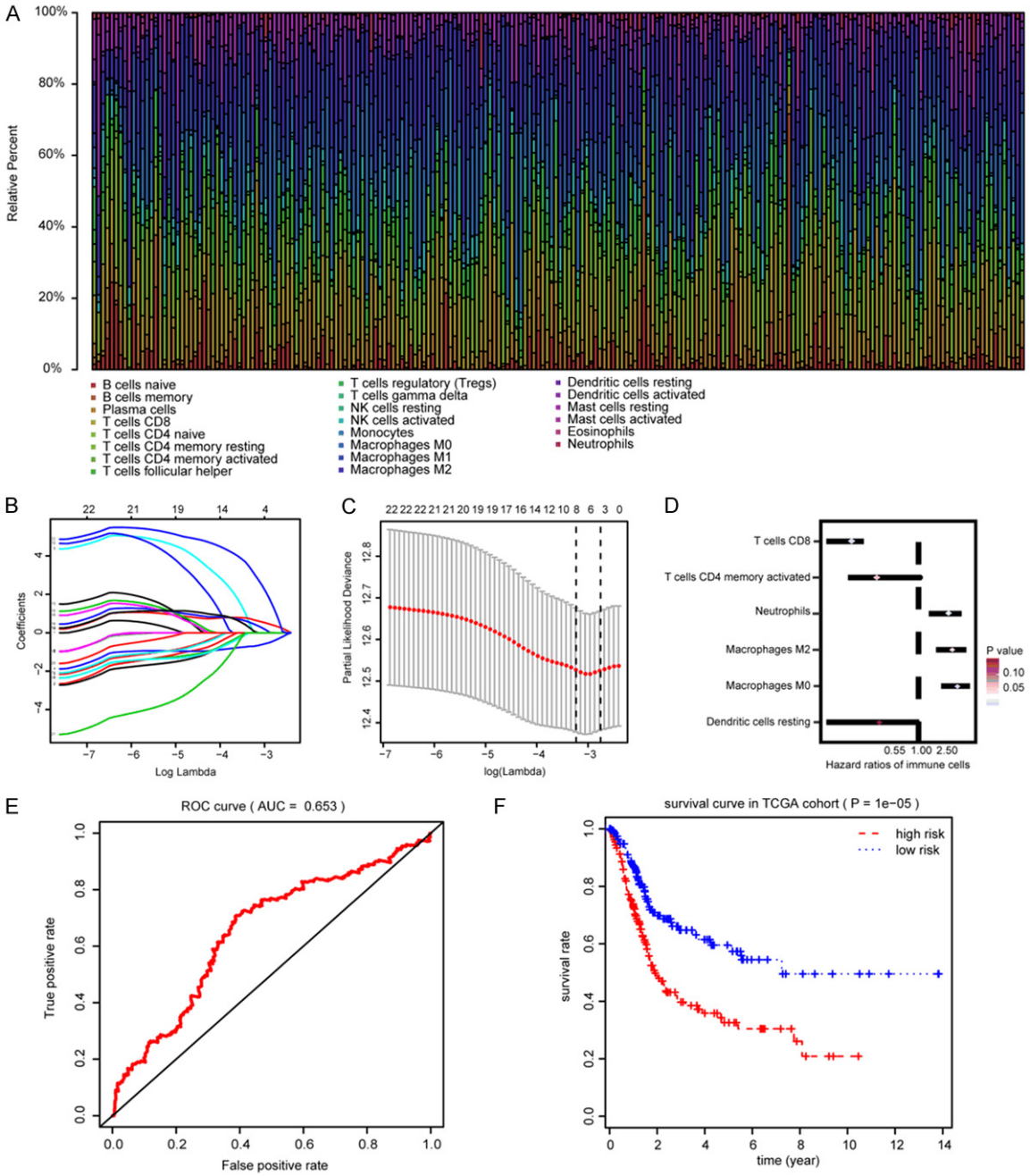

Figure 1. Identification of hub prognostic immune infiltrating cells and construction of TIICS model. A. Summary of 22 inferred immune cell subtypes by CIBERSORT algorithm. Bar charts exhibit the cell proportions and various annotated colors represent 22 immune cells. B. Cross-validation was performed for tuning parameter selection in the LASSO regression model. C. Illustration for LASSO coefficient profiles of 22 immune cells. LASSO, least absolute shrinkage and selection operator. D. Hazard ratios of 6 prognostic immune cells associated with OS by univariate Cox analysis. E. ROC curve of TIICS model for assessment of predictive accuracy. F. Comparisons of differential survival outcomes between two TIICS levels via Kaplan-Meier analysis with log-rank test.

TIICS correlated with clinical characteristics and validation in another cohort

The Wilcox rank-sum test or Kruskal-Wallis (K-W) test showed that high infiltrating levels of TIICS correlated with higher AJCC-TNM stages and advanced tumor grades in TCGA cohort (**Figure 3A-D**). To validate the significantly risk immune cells and TIICS, we obtained the 195 BLCA patients and constructed the TIICS

Table 2. Univariate Cox analysis for 22 immune infiltration cells in BLCA

Cell type	HR	Lower bund (95% CI)	Upper bound (95% CI)	*P* value
Macrophages M0	5.042	2.631	8.514	0.001
T cells CD8	0.093	0.013	0.282	0.004
Neutrophils	3.902	1.471	5.263	0.010
Macrophages M2	4.643	1.549	7.234	0.043
T cells CD4 memory activated	0.075	0.012	1.032	0.060
T cells follicular helper	0.087	0.022	1.093	0.106
T cells regulatory (Tregs)	0.131	0.021	1.216	0.132
T cells CD4 naive	34.949	0.812	53.193	0.140
Dendritic cells resting	0.221	0.023	1.072	0.152
Mast cells resting	5.370	0.917	10.329	0.192
B cells memory	0.070	0.011	1.215	0.277
NK cells resting	0.142	0.027	1.201	0.360
T cells gamma delta	96.105	0.971	183.427	0.394
Eosinophils	0.118	0.002	1.936	0.646
Dendritic cells activated	0.680	0.241	1.254	0.712
Plasma cells	0.808	0.671	2.103	0.825
NK cells activated	0.670	0.304	1.214	0.828
Mast cells activated	1.479	0.751	3.019	0.835
B cells naïve	0.853	0.613	1.273	0.889
Macrophages M1	1.126	0.271	3.067	0.913
Monocytes	1.060	0.439	2.107	0.982
T cells CD4 memory resting	1.002	0.701	2.051	0.998

through the same procedure (Table S3). In GSE13507, the TIICS level was associated with T stages (P=0.005) and tumor grades (P=0.004) (**Figure 3E**, **3F**). Moreover, the ROC curve showed the predictive value of TIICS with AUC=0.685, and patients with high TIICS levels suffered from poor prognostic outcomes (P=0.00162), which was in line with the results in the TCGA-BLCA cohorts (**Figure 3G**, **3H**).

Identification of 16 hub tumor immune infiltrating related signature

Since we investigated the prognostic immune cells in tumor microenvironment, we invented to further uncover the potential related signature that highly associated with TIICS and survival outcomes. Differential analysis between the two TIICS levels revealed a list of 497 significant genes with FDR <0.05 (Table S4; **Figure 4A**). Then, we screened out a total of 154 differential immune genes using the data from the ImmPort database (**Figure 4B**). Functional analysis based on the differentially expressed genes revealed the enriched immune-related GO items in **Table 3**, and the KEGG showed the top pathways that these signature might be involved in, including natural killer cell mediated cytotoxicity, cytokine-cytokine receptor interaction, and T cell receptor signaling pathways. Subsequently, the GSEA results demonstrated that there were several enriched immune-related pathways, including natural killer cell mediated cytotoxicity, B cell receptor signaling pathway, T cell receptor signaling pathway and pathways in cancer. Additionally, we utilized the univariate Cox regression method to screen the 74 significantly prognosis-related immune signature that correlated with TIICS (P<0.05). Stepwise algorithm was performed to identify the 16 key prognostic TIICS-related genes in **Table 4**.

Correlation of TIICS-related signature with infiltrating levels of immune cells

Using the TIMER database, we discussed the relationships of 16 hub signature with immune infiltration cells. From the Pearson coefficients and estimated *P* value, we observed that these signature were highly correlated with immune infiltration cells, especially including B cell, $CD8^+$ T cell, $CD4^+$ T cell, Macrophages, Neutrophil and Dendritic Cell (**Figure 5**). What is more, the mutants of these immune commonly led to lower infiltrating levels of immune cells consisted of $CD4^+$ T cell, Neutrophil and Dendritic cell (Figure S1).

Assessment of TIICS-related ISPI in BLCA and validation in GSE13507

Using the stepwise regression results, we established and calculated the immune signature related Prognostic Index (PI) for BLCA cohorts. Then, we classified the cases into two groups according to the cutoff value of the median value of PI. The distributions of vital

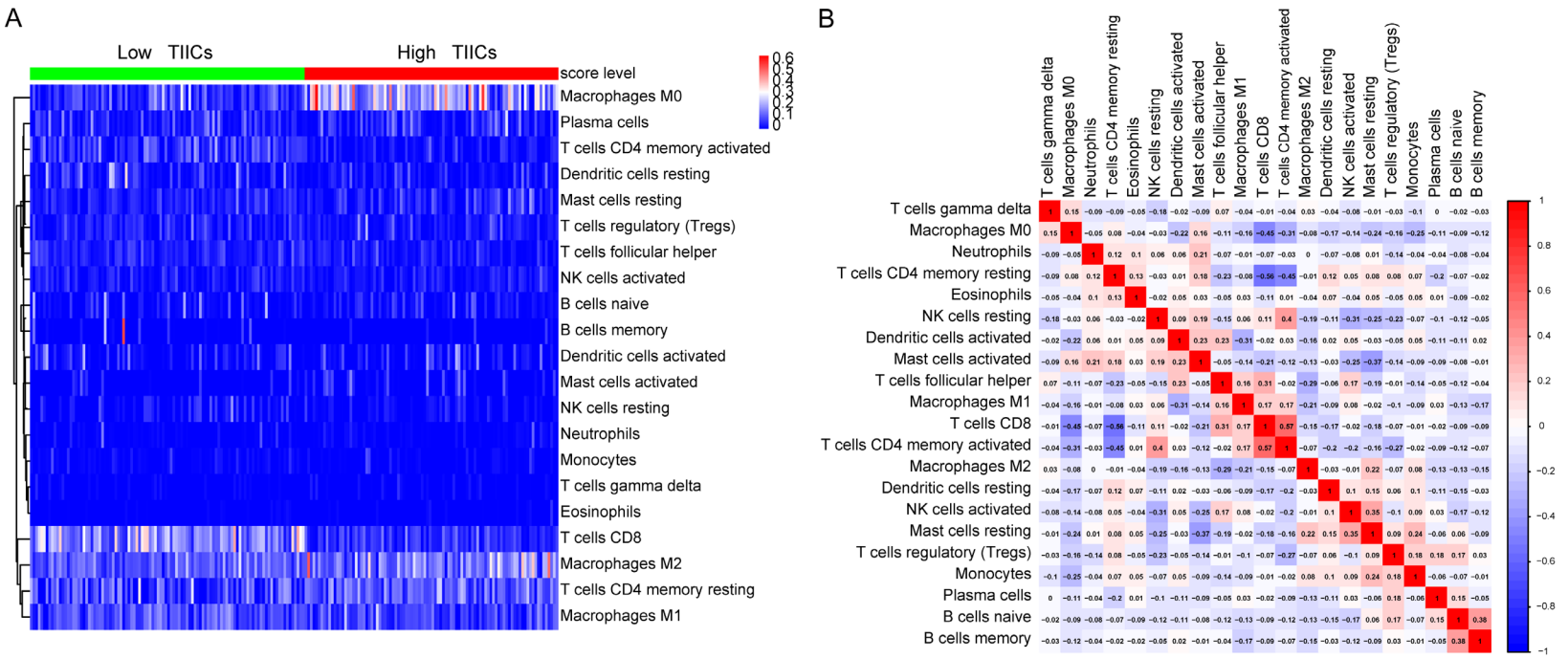
A
Low TIICs
High TIICs
score level
Macrophages M0
Plasma cells
T cells CD4 memory activated
Dendritic cells resting
Mast cells resting
T cells regulatory (Tregs)
T cells follicular helper
NK cells activated
B cells naive
B cells memory
Dendritic cells activated
Mast cells activated
NK cells resting
Neutrophils
Monocytes
T cells gamma delta
Eosinophils
T cells CD8
Macrophages M2
T cells CD4 memory resting
Macrophages M1
B
T cells gamma delta
Macrophages M0
Neutrophils
T cells CD4 memory resting
Eosinophils
NK cells resting
Dendritic cells activated
Mast cells activated
T cells follicular helper
Macrophages M1
T cells CD8
T cells CD4 memory activated
Macrophages M2
Dendritic cells resting
NK cells activated
Mast cells resting
T cells regulatory (Tregs)
Monocytes
Plasma cells
B cells naive
B cells memory

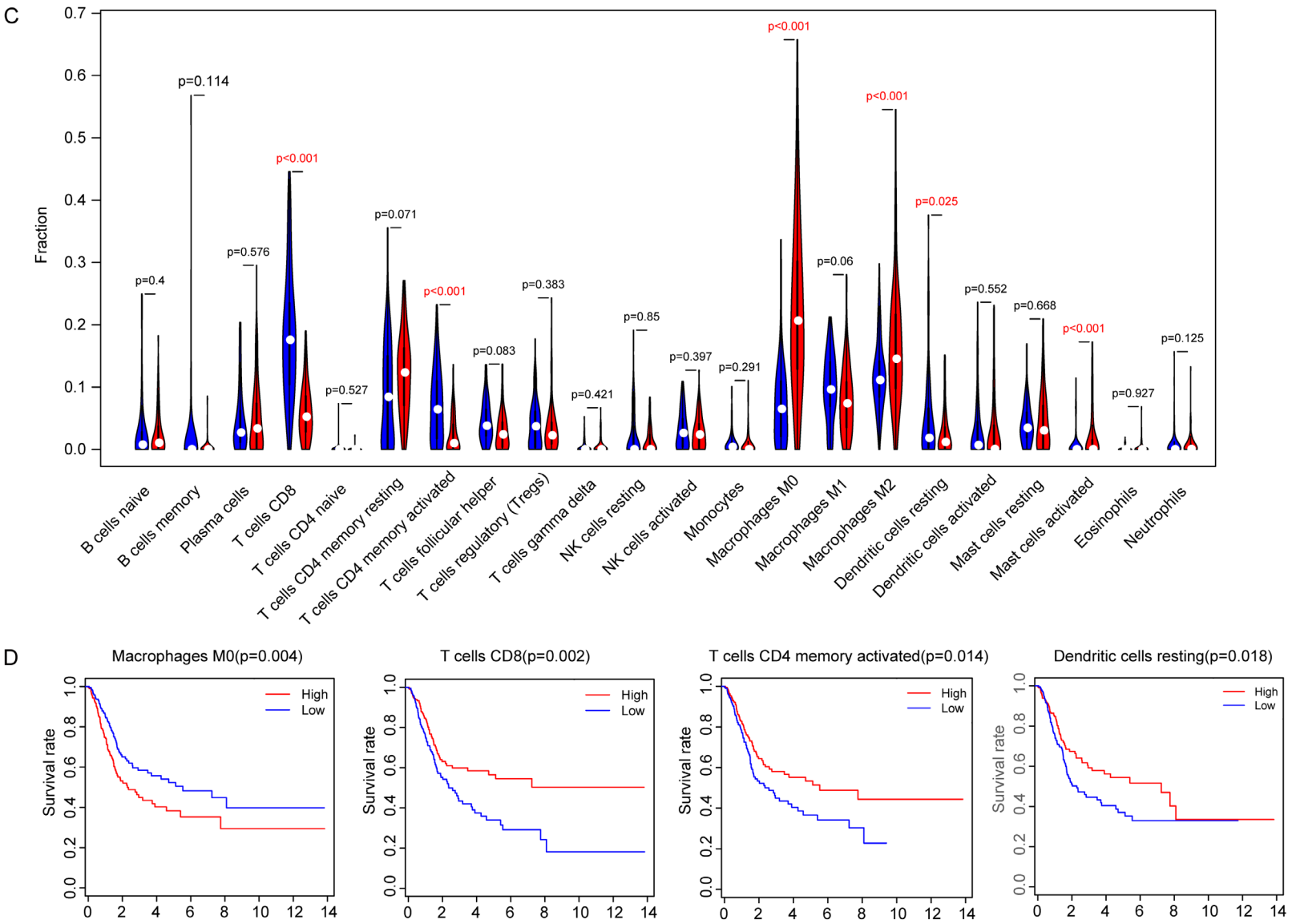

Figure 2. Depiction and distributions of immune cells in two TIICs groups. A. Differential abundance of immune cells in two TIICS groups in heatmap plot. B. Correlation heatmap represents the coincident and exclusive associations across 22 immune cells, where blue represents the mutual exclusion and red represents the consistence ranging from -1 to 1. C. Differential density of immune cells in two TIICS groups was compared by Wilcox rank-sum test. D. Survival analysis of immune

cells was conducted, where higher level of M0 macrophage correlated with poor outcomes and lower level of $CD8^+$ T cell, memory activated $CD4^+$ T cells, resting Dendritic cells were associated with worse prognosis.

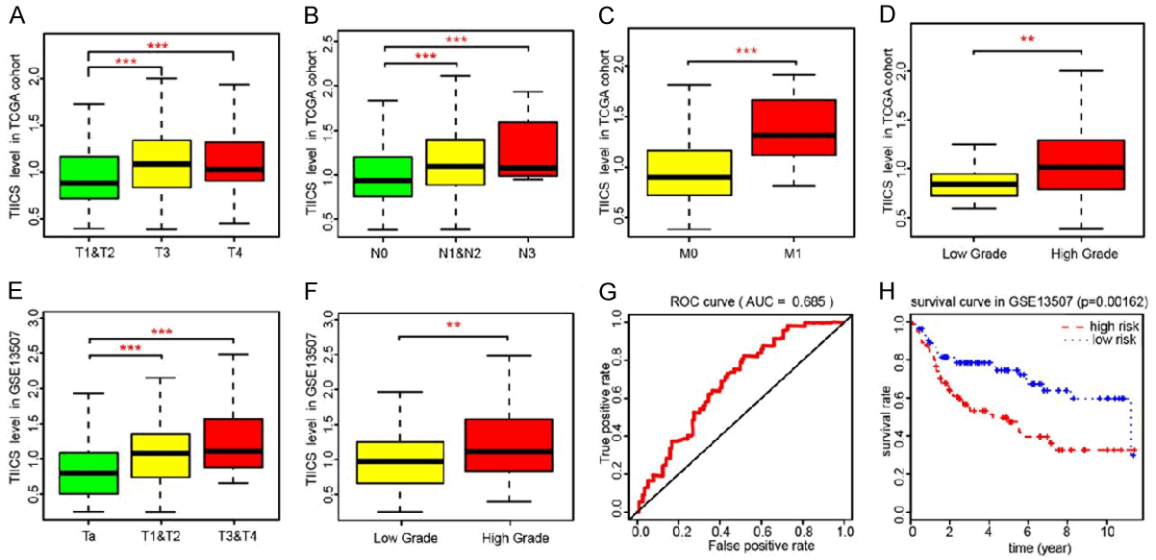

Figure 3. Correlation analysis of TIICS with clinical characteristics and validation in an independent dataset. A-D. Non-parametric test indicated that higher TIICS level correlated with higher AJCC-TNM stages and advanced tumor grades in TCGA cohorts. E, F. Similar results were also observed in GSE13507, where higher TIICS levels also correlated with higher T stages and tumor grades. The * represented the P<0.05. The ** represented the P<0.01, and *** represented the P<0.001. G, H. TIICS model was validated in GSE13507, of which the AUC was 0.685 and the patients with higher TIICS model showed less survival time (P=0.00162).

status in two groups were shown in **Figure 7A**. The ROC curve showed the superior predictive accuracy of PI in 3-year overall survival prediction with AUC=0.797 (**Figure 7B**). Patients with higher PI showed poor prognosis relative to those with low PI (P=0, **Figure 7C**). In the validation group, the PI was demonstrated to be an independent factor (AUC=0.673) and the *P* value in Kaplan-Meier analysis was 1e-05 in survival plot (**Figure 7E**, **7F**).

Discussion

Patients diagnosed with BLCA have a difficult decision between radical cystectomy and trimodal therapy consisted of maximal transurethral resection of tumor followed by chemotherapy, and close cystoscopic surveillance [21, 22]. The current evidence showed no advantage for one or other approaches in regard to survival outcomes [23]. With the breakthrough of immune therapy in recent years, PD1/PDL-1 antibody or other novel immune drugs have been recommended for clinical use and nearly replaced chemotherapy, becoming a highly promising role in the management of high-grade non-muscle-invasive bladder cancer (NIMBC) [24]. However, there existed problems that some BLCA patients showed less effective to immunotherapy due to tumor heterogeneity or other indefinite resistant mechanisms [25-27]. Given the importance of immune environment in the promotion of tumorigenesis, it is significant to identify immune cells or related signature to predict prognosis or served as potential targets in immune treatment [28-30]. Although gene signature for prognosis of tumors based on non-coding RNAs, ceRNAs or mRNA were commonly explored and reported, characterization of prognostic immune cell subtypes combined with immune signature analysis for BLCA have been less investigated.

In our study, this is the first attempt to explore a genome-wide profiling study to uncover risk tumor infiltrating immune cells, immune signature and their clinical significance across multiple databases. We obtained mRNA profiles of 408 BLCA matched with 25 normal tissues from TCGA database and identified 6 prognostic immune infiltration cells associated with survival via LASSO method and Cox regression model. Subsequently, a robust TIICS model was constructed and differential analysis was performed between two TIICS

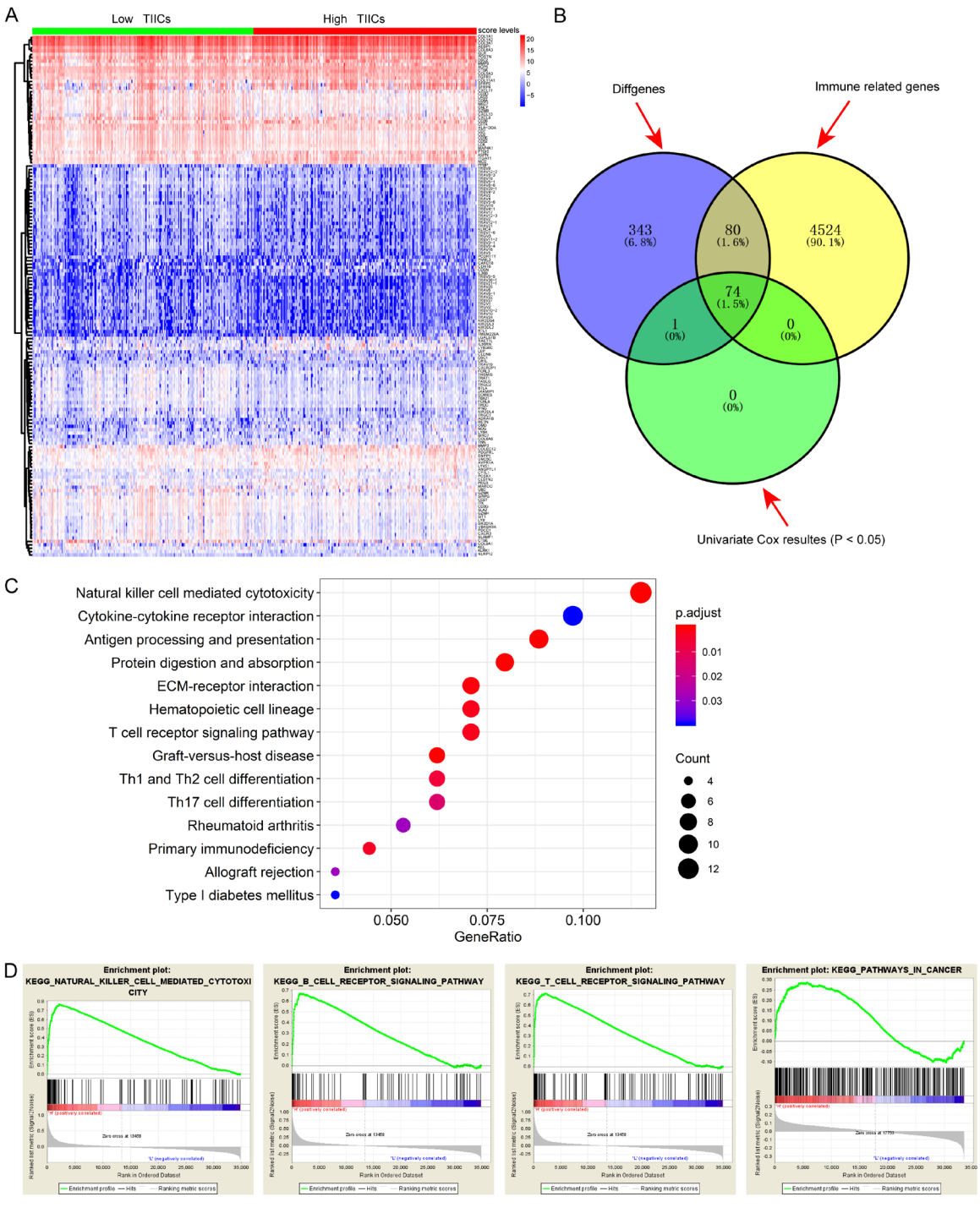

Figure 4. Identification of hub TIICS-related immune signature and functional analysis. A. Differentially expressed genes (DEGs) between two TIICS groups with |log (Fold Change)| >1 and false discovery rate (FDR) <0.05 as the cutoff value. B. Identification of hub immune signature via intersection and Cox analysis. C. Top immune-related crosstalk that these DEGs might be involved in. D. GSEA for comparing immune phenotype between high- and low-TIICS groups.

levels to further discover significant TIICS related immune signature. Correlation analysis revealed that TIICS level was associated with higher tumor grades, advanced pathological stages and AJCC-TNM stages positively. Kaplan-Meier analysis also indicated the associations between TIICS and OS, where patients in high-risk group showed significantly worse

Table 3. Significantly top 30 enriched GO items of differentially expressed genes between two TIICS levels

Ontology	Description	*P* value
GOTERM_BP_DIRECT	T cell activation	6.57E-07
	extracellular structure organization	8.60E-07
	extracellular matrix organization	9.25E-07
	T cell differentiation	1.59E-05
	collagen fibril organization	3.50E-05
	cellular defense response	0.000134
	T cell receptor signaling pathway	0.000231
	positive T cell selection	0.000252
	extracellular matrix disassembly	0.000575
	lymphocyte differentiation	0.000696
GOTERM_MF_DIRECT	extracellular matrix structural constituent	4.46E-10
	MHC protein binding	2.85E-07
	extracellular matrix structural constituent conferring tensile strength	2.85E-07
	collagen binding	4.11E-06
	serine-type peptidase activity	4.20E-05
	serine hydrolase activity	4.29E-05
	serine-type endopeptidase activity	4.54E-05
	fibronectin binding	0.001746
	metalloendopeptidase activity	0.001746
	receptor ligand activity	0.002964
GOTERM_CC_DIRECT	endoplasmic reticulum lumen	0.026267
	lysosomal lumen	0.018802
	extracellular matrix component	0.000321
	T cell receptor complex	0.000157
	complex of collagen trimers	1.20E-05
	external side of plasma membrane	7.43E-07
	collagen trimer	6.15E-07
	fibrillar collagen trimer	3.65E-07
	banded collagen fibril	3.65E-07
	collagen-containing extracellular matrix	7.80E-08

survival outcomes than that in low-risk group. We further validated the TIICS model using the 165 BLCA patients from the GSE13507 series, in accordance with previous results. TIMER database is a web server that used to conduct comprehensive analysis of tumor-infiltrating immune cells. The Pearson coefficients between identified immune signature and hub immune cells further analyze the relationships among them. However, the specific regulations across the signature and immune cell subtypes were warranted for further experimental validation.

Numerous previous data have demonstrated that tumor associated macrophages (TAMs) density correlated with poor survival in multiple cancers, promoting tumor progression or metastasis by directly affecting the epithelial-mesenchymal transition (EMT), angiogenesis, and immune escape [31-35]. Chen C et al. have reported that LNMAT1 overexpression led to lymphatic nodes metastasis in BLCA, by inducing the recruitment of macrophage in tumor microenvironment with CCL2/TAMs axis. In our research, we identified that specific subtype M0 macrophage was associated with poor prognosis (HR=5.042, P=0.001), which especially accounted for higher fractions in tumor samples. Another immune risk cells, M0 macrophage, was also found to be related with survival (HR=4.643, P=0.043) in Cox regres-

Table 4. Identification of 16 hub prognostic TIICS-related signature based on stepwise regression method

Genesymbol	Description	coef	exp (coef)	se (coef)	P
COL1A2	collagen type I alpha 2 chain	0.45407	1.5747	0.19329	0.018815
COL3A1	collagen type III alpha 1 chain	-0.36841	0.69183	0.22804	0.106194
CTSE	cathepsin E	-0.05875	0.94294	0.02553	0.021389
CXCL13	C-X-C motif chemokine ligand 13	-0.09092	0.91309	0.05276	0.084821
DSC1	desmocollin 1	0.08462	1.0883	0.04128	0.040375
ISLR	immunoglobulin superfamily containing leucine rich repeat	0.1515	1.16358	0.09388	0.106567
KLRK1	killer cell lectin like receptor K1	-0.24256	0.78462	0.06882	0.000424
MAP4K1	mitogen-activated protein kinase kinase kinase kinase 1	-0.20795	0.81225	0.11687	0.075195
NID2	nidogen 2	0.17214	1.18784	0.10616	0.104912
SFRP2	secreted frizzled related protein 2	0.10644	1.11231	0.05029	0.034297
UBASH3A	ubiquitin associated and SH3 domain containing A	0.37533	1.45548	0.13421	0.005163
CYTL1	cytokine like 1	0.11834	1.12563	0.05877	0.044057
COL1A1	collagen type I alpha 1 chain	-0.46361	0.62901	0.24535	0.058809
KIR2DS4	killer cell immunoglobulin like receptor, two Ig domains and short cytoplasmic tail 4	-0.10597	0.89945	0.06575	0.107022
CD3G	CD3g molecule	-0.19408	0.82359	0.12124	0.109419
CD36	CD36 molecule	0.05202	1.05339	0.03453	0.131996

sion analysis. However, no significance was observed in subsequent Kaplan-Meier curves and larger samples were needed to evaluate again. Additionally, it is robust to note that we also observed the $CD8^+$ T cell and memory B cell infiltration had relationships with prognosis, where the factions of $CD8^+$ T cell and memory activated $CD4^+$ T cells showed lower infiltrates in tumor samples versus normal and indicated poor survival outcomes. $CD8^+$ T cell and activated $CD4^+$ T cells were already acknowledged as important components in cellular immunity and plays a major suppressor role in various tumor micro-environment, including breast cancer, clear cell renal cell carcinoma or colorectal cancer. Moreover, Fu H et al. have recently confirmed five significant immune infiltrates ($CD8^+$ T cell, Macrophage, NK, Treg, Mast Cell) and successfully classified the patients into A and B immunotypes using the LASSO method based on TCGA cohort plus with 258 MIBC patients from local hospital. In accordance with these researches, our results predicted that higher infiltrating density of $CD8^+$ T cell and activated $CD4^+$ T cells conferred prolonged OS and better prognosis, providing a future therapeutic target in BLCA.

Apart from the detailed assessment of immune infiltration in BLCA, we also discussed the TIICS related immune signature for OS prediction consisted of 16 prognostic immune genes (KLRK1, UBASH3A, COL1A2, CTSE, SFRP2, DSC1, CYTL1, COL1A1, MAP4K1, CXCL13, NID2, COL3A1, ISLR, KIR2DS4, CD3G, CD36). Among these identified genes, we found that most of them were cytokines or chemokines, functioning as vital components in tumor immunity. COL1A1, COL1A2, COL3A1 were members of collagen factors and they were commonly reported, especially the COL1A1, in promotion of tumorigenesis or metastasis across multiple tumors including breast cancer, gastric cancer and cervical cancer. Functional analysis suggested that differentially expressed genes might be involved in cytokine-cytokine receptor interaction, natural killer cell mediated cytotoxicity, ECM-receptor interaction and other important immune crosstalk. Besides, the GSEA and mutation analysis of signature based on TIMER database further strengthened the tight relationships between signature and immune infiltrates, especially $CD4^+$ T cell, neutrophil and dendritic cell (**Figure 4D**; Figure S1). Kaplan-Meier analysis demonstrated the prognostic value of immune signature and we selected some to exhibit in **Figure 6**. It is worthy to note that these genes possessed well predictive value, and the PI showed robust stability in discovery and validation group. Given the potential associations with immune infiltrates, these genes deserved for further functional validation and exploration on therapeutic targets.

Hazard infiltrating immune cells in bladder urothelial carcinoma

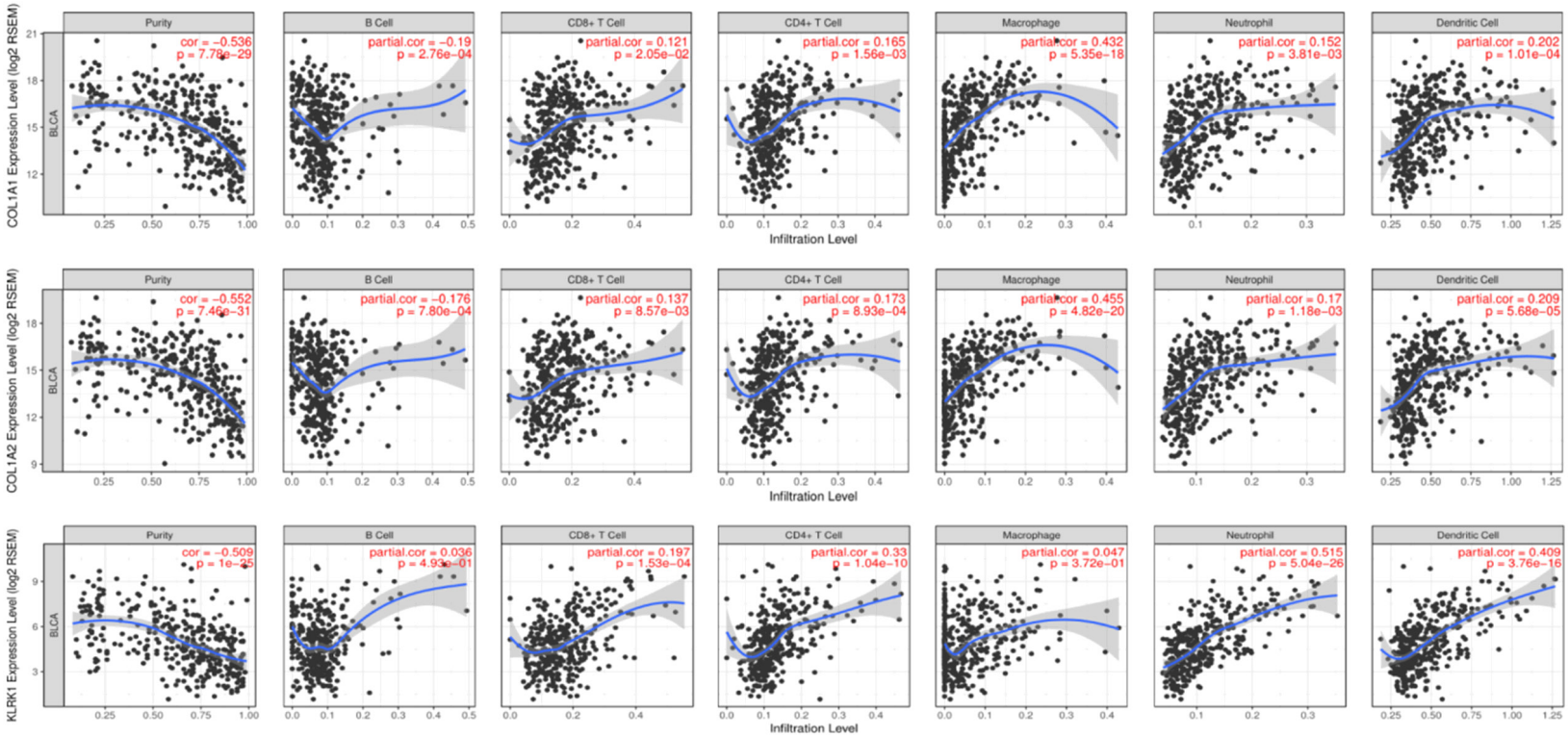

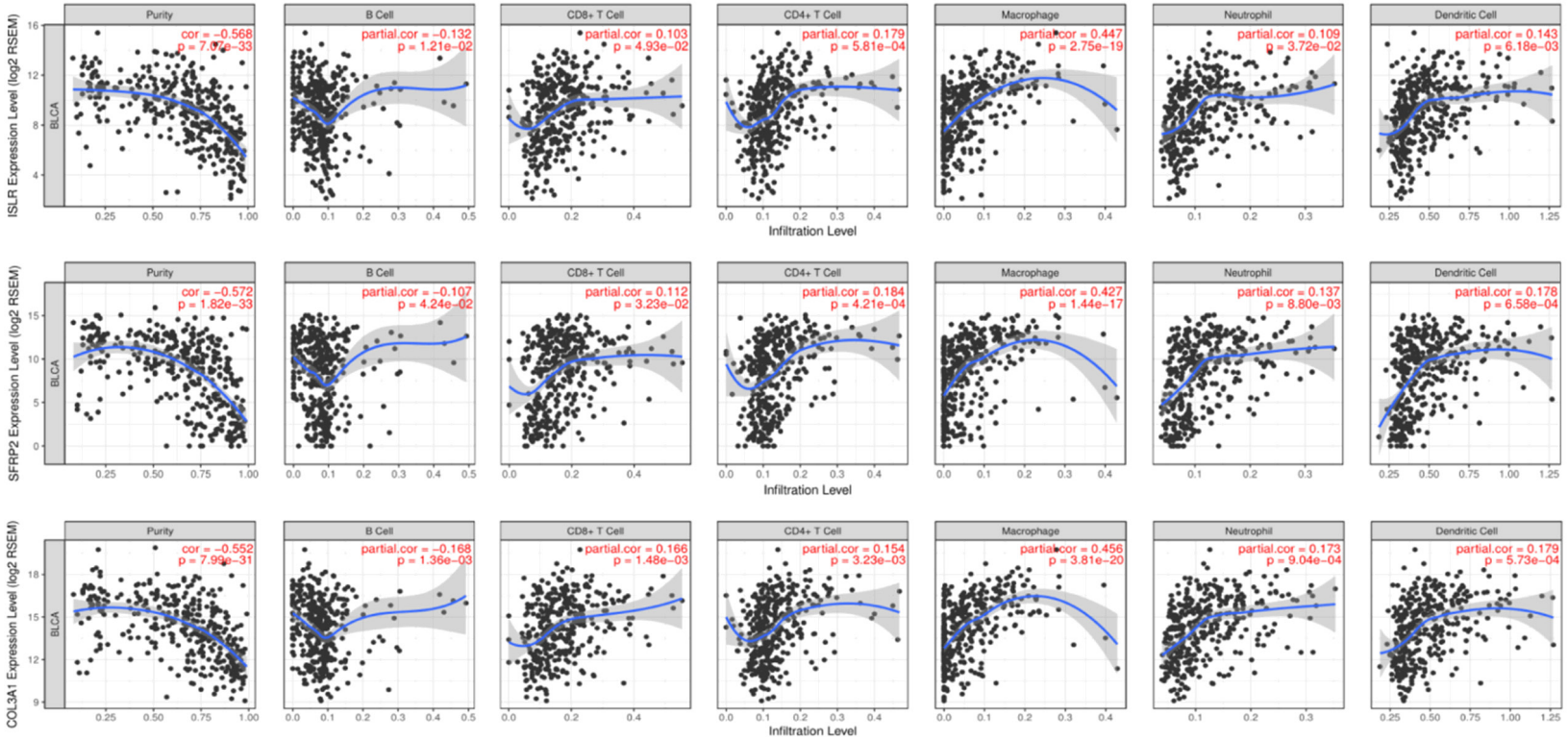

Figure 5. Correlation of hub prognostic TIICS-related signature with immune infiltration level in BLCA based on TIMER database.

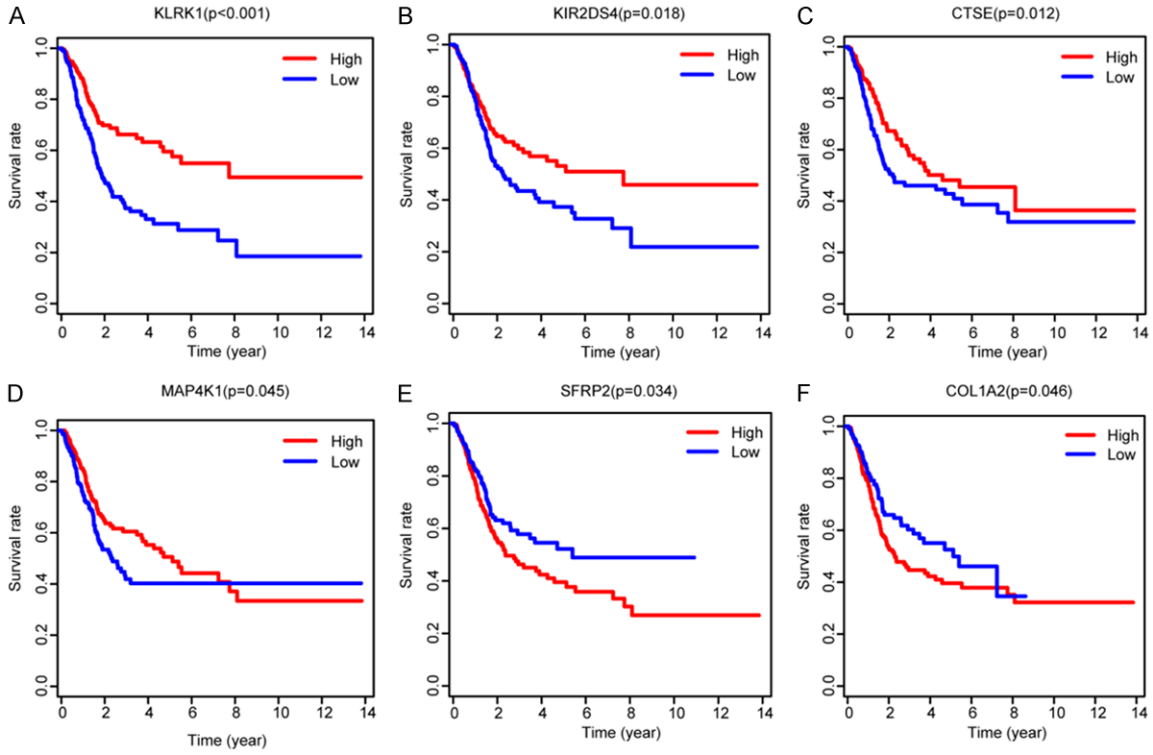

Figure 6. Kaplan-Meier analysis with log-rank test of hub immune signature and selected some to exhibit.

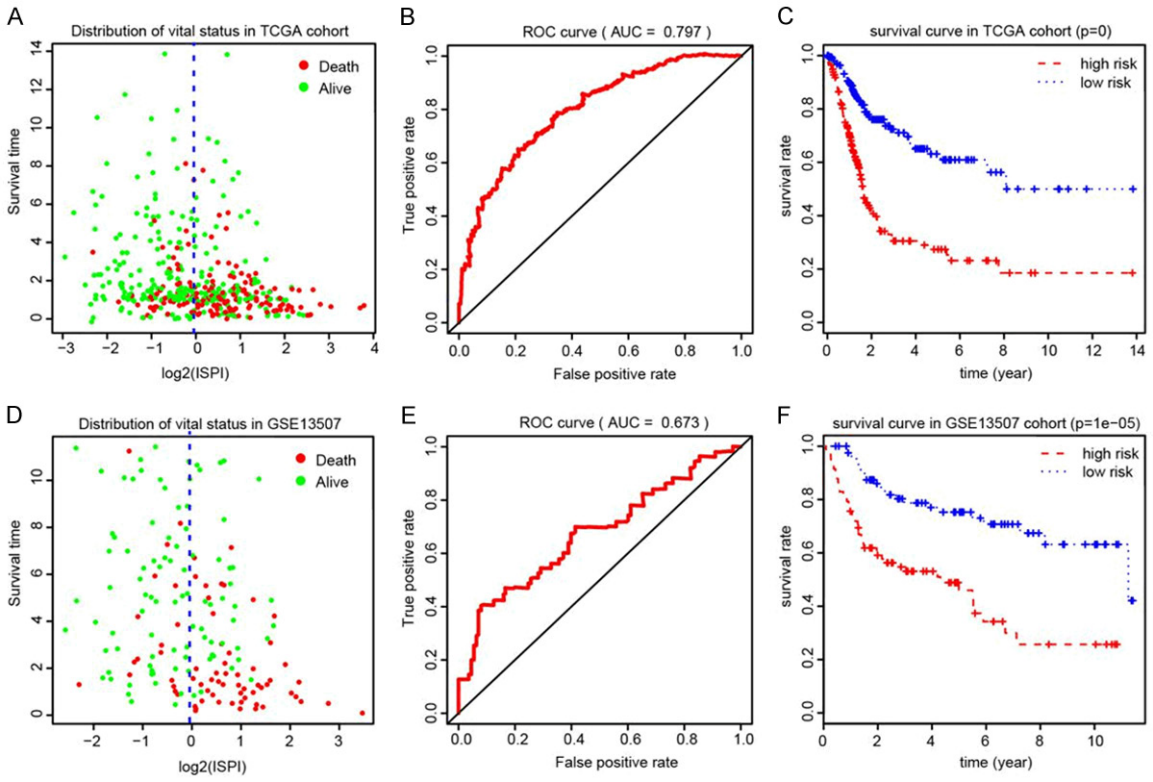

Figure 7. Construction and evaluation of ISPI based on 16 hub signature for BLCA. A. The distribution of vital status of patients in two ISPI groups. B. The AUC of ROC curve was 0.797 showing superior predictive accuracy. C. Patients with higher level of ISPI demonstrated poor outcomes (P<0.001). D-F. Validation of the robust ISPI model in GSE13507.

However, there are still several defects in our research that need to be further improved. First, the modest inconsistent results of Cox regression analysis versus Kaplan-Meier analysis of M2 Macrophages, memory activated $CD4^+$ T cells and resting Dendritic cells might need larger samples to further investigate. Secondly, since we have identified the relationships between TIICS related signature with immune infiltrates, the functional analysis should be added to uncover underlying specific regulatory mechanisms. In addition, although we utilized the GSE13507 cohort as the validation group, there is still a lack of multi-center large clinical samples to make sure the predictive accuracy of TIICS model. Last, flow cytometry might be warranted to further evaluate the fractions of immune cells, which was an important supplementary work for CIBERSORT algorithm.

Taken together, immune research has already attracted the intensive attention in cancer study. The present work including 573 BLCA samples have identified a robust TIICS model consisted of 6 immune cells and discussed the TIICS-related immune signature for OS prediction. This is our first attempt to implement the integrated omic analysis of immune landscape from genomic signature to immune infiltrates based on high throughput data with corresponding clinical information from large samples, which providing valuable suggestions on risk prediction or individualized immunotherapy.

Acknowledgements

This study was supported by the Guangdong Provincial Natural Science Foundation (2018-A030313434), The Guangdong Provincial Medical Science Research Foundation (A2018-259), and the Guangzhou Municipal Science and Technology Program (201904010006).

Disclosure of conflict of interest

None.

Address correspondence to: Peng Zhang, Organ Transplant Center, The Second Affiliated Hospital of Guangzhou Medical University, No. 63 South Asian Games Road, Panyu District, Guangzhou 511447, Guangdong Province, China. Tel: +86-020-39195871; E-mail: 410313386@qq.com

References

[1] Bidnur S, Savdie R and Black PC. Inhibiting immune checkpoints for the treatment of bladder cancer. Bladder Cancer 2016; 2: 15-25.

[2] Fakhrejahani F, Tomita Y, Maj-Hes A, Trepel JB, De Santis M and Apolo AB. Immunotherapies for bladder cancer: a new hope. Curr Opin Urol 2015; 25: 586-596.

[3] Carneiro BA, Meeks JJ, Kuzel TM, Scaranti M, Abdulkadir SA and Giles FJ. Emerging therapeutic targets in bladder cancer. Cancer Treat Rev 2015; 41: 170-178.

[4] Anantharaman A, Friedlander T, Lu D, Krupa R, Premasekharan G, Hough J, Edwards M, Paz R, Lindquist K, Graf R, Jendrisak A, Louw J, Dugan L, Baird S, Wang YP, Dittamore R and Paris PL. Programmed death-ligand 1 (PD-L1) characterization of circulating tumor cells (CTCs) in muscle invasive and metastatic bladder cancer patients. BMC Cancer 2016; 16: 744.

[5] Chism DD. Urothelial carcinoma of the bladder and the rise of immunotherapy. J Natl Compr Canc Netw 2017; 15: 1277-1284.

[6] Ferreira-Teixeira M, Paiva-Oliveira D, Parada B, Alves V, Sousa V, Chijioke O, Münz C, Reis F, Rodrigues-Santos P and Gomes C. Natural killer cell-based adoptive immunotherapy eradicates and drives differentiation of chemoresistant bladder cancer stem-like cells. BMC Med 2016; 14: 163.

[7] Choudhury NJ, Kiyotani K, Yap KL, Campanile A, Antic T, Yew PY, Steinberg G, Park JH, Nakamura Y and O'Donnell PH. Low T-cell receptor diversity, high somatic mutation burden, and high neoantigen load as predictors of clinical outcome in muscle-invasive bladder cancer. Eur Urol Focus 2016; 2: 445-452.

[8] Kardos J, Chai S, Mose LE, Selitsky SR, Krishnan B, Saito R, Iglesia MD, Milowsky MI, Parker JS, Kim WY and Vincent BG. Claudin-low bladder tumors are immune infiltrated and actively immune suppressed. JCI Insight 2016; 1: e85902.

[9] Zhou TC, Sankin AI, Porcelli SA, Perlin DS, Schoenberg MP and Zang X. A review of the PD-1/PD-L1 checkpoint in bladder cancer: from mediator of immune escape to target for treatment. Urol Oncol 2017; 35: 14-20.

[10] Ghasemzadeh A, Bivalacqua TJ, Hahn NM and Drake CG. New strategies in bladder cancer: a second coming for immunotherapy. Clin Cancer Res 2016; 22: 793-801.

[11] Chen X, Jin Y, Gong L, He D, Cheng Y, Xiao M, Zhu Y, Wang Z and Cao K. Bioinformatics analysis finds immune gene markers related to the prognosis of bladder cancer. Front Genet 2020; 11: 607.

[12] Goodwin Jinesh G, Willis DL and Kamat AM. Bladder cancer stem cells: biological and therapeutic perspectives. Curr Stem Cell Res Ther 2014; 9: 89-101.
[13] Kates M, Sopko NA, Matsui H, Drake CG, Hahn NM and Bivalacqua TJ. Immune checkpoint inhibitors: a new frontier in bladder cancer. World J Urol 2016; 34: 49-55.
[14] Piao XM, Byun YJ, Kim WJ and Kim J. Unmasking molecular profiles of bladder cancer. Investig Clin Urol 2018; 59: 72-82.
[15] Chen JB, Zhu YW, Guo X, Yu C, Liu PH, Li C, Hu J, Li HH, Liu LF, Chen MF, Chen HQ and Xiong-Bing Z. Microarray expression profiles analysis revealed lncRNA OXCT1-AS1 promoted bladder cancer cell aggressiveness via miR-455-5p/JAK1 signaling. J Cell Physiol 2019; 234: 13592-13601.
[16] Kim J, Akbani R, Creighton CJ, Lerner SP, Weinstein JN, Getz G and Kwiatkowski DJ. Invasive bladder cancer: genomic insights and therapeutic promise. Clin Cancer Res 2015; 21: 4514-4524.
[17] Le Goux C, Damotte D, Vacher S, Sibony M, Delongchamps NB, Schnitzler A, Terris B, Zerbib M, Bieche I and Pignot G. Correlation between messenger RNA expression and protein expression of immune checkpoint-associated molecules in bladder urothelial carcinoma: a retrospective study. Urol Oncol 2017; 35: 257-263.
[18] Masson-Lecomte A, Rava M, Real FX, Hartmann A, Allory Y and Malats N. Inflammatory biomarkers and bladder cancer prognosis: a systematic review. Eur Urol 2014; 66: 1078-1091.
[19] Sjödahl G, Lövgren K, Lauss M, Chebil G, Patschan O, Gudjonsson S, Månsson W, Fernö M, Leandersson K, Lindgren D, Liedberg F and Höglund M. Infiltration of CD3(+) and CD68(+) cells in bladder cancer is subtype specific and affects the outcome of patients with muscle-invasive tumors. Urol Oncol 2014; 32: 791-797.
[20] Kates M, Nirschl T, Sopko NA, Matsui H, Kochel CM, Reis LO, Netto GJ, Hoque MO, Hahn NM, McConkey DJ, Baras AS, Drake CG and Bivalacqua TJ. Intravesical BCG induces CD4(+) T-cell expansion in an immune competent model of bladder cancer. Cancer Immunol Res 2017; 5: 594-603.
[21] Huang J, Lo UG, Wu S, Wang B, Pong RC, Lai CH, Lin H, He D, Hsieh JT and Wu K. The roles and mechanism of IFIT5 in bladder cancer epithelial-mesenchymal transition and progression. Cell Death Dis 2019; 10: 437.
[22] Mo Q, Nikolos F, Chen F, Tramel Z, Lee YC, Hayashi K, Xiao J, Shen J and Chan KS. Prognostic power of a tumor differentiation gene signature for bladder urothelial carcinomas. J Natl Cancer Inst 2018; 110: 448-459.
[23] Rosenberg JE, Hoffman-Censits J, Powles T, van der Heijden MS, Balar AV, Necchi A, Dawson N, O'Donnell PH, Balmanoukian A, Loriot Y, Srinivas S, Retz MM, Grivas P, Joseph RW, Galsky MD, Fleming MT, Petrylak DP, Perez-Gracia JL, Burris HA, Castellano D, Canil C, Bellmunt J, Bajorin D, Nickles D, Bourgon R, Frampton GM, Cui N, Mariathasan S, Abidoye O, Fine GD and Dreicer R. Atezolizumab in patients with locally advanced and metastatic urothelial carcinoma who have progressed following treatment with platinum-based chemotherapy: a single-arm, multicentre, phase 2 trial. Lancet 2016; 387: 1909-1920.
[24] Pettenati C and Ingersoll MA. Mechanisms of BCG immunotherapy and its outlook for bladder cancer. Nat Rev Urol 2018; 15: 615-625.
[25] Long X, Xiong W, Zeng X, Qi L, Cai Y, Mo M, Jiang H, Zhu B, Chen Z and Li Y. Cancer-associated fibroblasts promote cisplatin resistance in bladder cancer cells by increasing IGF-1/ER-beta/Bcl-2 signalling. Cell Death Dis 2019; 10: 375.
[26] Pichler R, Fritz J, Zavadil C, Schafer G, Culig Z and Brunner A. Tumor-infiltrating immune cell subpopulations influence the oncologic outcome after intravesical bacillus calmette-guerin therapy in bladder cancer. Oncotarget 2016; 7: 39916-39930.
[27] Ratner M. Genentech's PD-L1 agent approved for bladder cancer. Nat Biotechnol 2016; 34: 789-790.
[28] Wu L, Zhang M, Qi L, Zu X, Li Y, Liu L, Chen M, Li Y, He W, Hu X, Mo M, Ou Z and Wang L. ERalpha-mediated alterations in circ_00236-42 and miR-490-5p signaling suppress bladder cancer invasion. Cell Death Dis 2019; 10: 635.
[29] Ren R, Tyryshkin K, Graham CH, Koti M and Siemens DR. Comprehensive immune transcriptomic analysis in bladder cancer reveals subtype specific immune gene expression patterns of prognostic relevance. Oncotarget 2017; 8: 70982-71001.
[30] Knollman H, Godwin JL, Jain R, Wong YN, Plimack ER and Geynisman DM. Muscle-invasive urothelial bladder cancer: an update on systemic therapy. Ther Adv Urol 2015; 7: 312-330.
[31] Sfakianos JP and Galsky MD. Neoadjuvant chemotherapy in the management of muscle-invasive bladder cancer: bridging the gap between evidence and practice. Urol Clin North Am 2015; 42: 181-187.
[32] Zhang H, Prado K, Zhang KX, Peek EM, Lee J, Wang X, Wang X, Huang J, Li G, Pellegrini M and Chin AI. Biased expression of the FOXP-3delta3 isoform in aggressive bladder cancer

mediates differentiation and cisplatin chemotherapy resistance. Clin Cancer Res 2016; 22: 5349-5361.

[33] Lázaro M, Gallardo E, Doménech M, Pinto Á, González-del-Alba A, Del Alba AG, Puente J, Fernández O, Font A, Lainez N and Vázquez S. SEOM clinical guideline for treatment of muscle-invasive and metastatic urothelial bladder cancer (2016). Clin Transl Oncol 2016; 18: 1197-1205.

[34] Singh P and Black P. Emerging role of checkpoint inhibition in localized bladder cancer. Urol Oncol 2016; 34: 548-555.

[35] Mitra AP and Lerner SP. Potential role for targeted therapy in muscle-invasive bladder cancer: lessons from the cancer genome atlas and beyond. Urol Clin North Am 2015; 42: 201-215.

Table S2. Calculation of TIICs for 408 BLCA patients in TCGA cohort

id	grade	stage	T	M	N	TIICs
TCGA-2F-A9KO	High Grade	Stage IV	T3	M0	N1	0.683920304
TCGA-2F-A9KP	High Grade	Stage IV	T3a	MX	N2	0.883436088
TCGA-2F-A9KQ	High Grade	Stage III	T3a	M0	N0	0.93463941
TCGA-2F-A9KR	High Grade	Stage III	T3a	M0	N0	0.817450142
TCGA-2F-A9KT	High Grade	Stage II	T2b	M0	N0	1.356010115
TCGA-2F-A9KW	High Grade	Stage III	T3b	MX	N0	1.834153452
TCGA-4Z-AA7M	High Grade	Stage III	T3a	M0	N0	1.439521732
TCGA-4Z-AA7N	High Grade	Stage III	T3a	M0	N0	0.918089037
TCGA-4Z-AA7O	High Grade	Stage II	T2a	M0	N0	0.769649779
TCGA-4Z-AA7Q	High Grade	Stage III	T3a	M0	NX	0.705648474
TCGA-4Z-AA7R	High Grade	Stage IV	T4b	M0	N0	1.443399834
TCGA-4Z-AA7S	High Grade	Stage III	T4a	M0	N0	1.05670457
TCGA-4Z-AA7W	High Grade	Stage II	T2a	M0	N0	0.526397804
TCGA-4Z-AA7Y	High Grade	Stage II	T2a	M0	N0	0.59456785
TCGA-4Z-AA80	High Grade	Stage II	T2a	M0	N0	0.829935732
TCGA-4Z-AA81	High Grade	Stage II	T2b	M0	N0	0.500544767
TCGA-4Z-AA82	High Grade	Stage IV	T2a	M0	N1	0.776417775
TCGA-4Z-AA83	High Grade	Stage II	T2a	M0	N0	1.320437336
TCGA-4Z-AA84	High Grade	Stage IV	T3a	M1	N2	1.409568101
TCGA-4Z-AA86	High Grade	Stage IV	T3a	M0	N1	1.086230465
TCGA-4Z-AA87	High Grade	Stage III	T4a	M0	N0	0.675161901
TCGA-4Z-AA89	High Grade	Stage IV	T4b	M0	N0	0.854195461
TCGA-5N-A9KI	High Grade	Stage III	T4	MX	NX	1.563734587
TCGA-5N-A9KM	High Grade	Stage III	T4a	MX	N0	0.740698316
TCGA-BL-A0C8	High Grade	Stage I	T1	M0	NX	1.363869489
TCGA-BL-A13I	High Grade	Stage III	T3	M0	N0	2.001884188
TCGA-BL-A13J	High Grade	Stage IV	T4	M0	N2	1.317075105
TCGA-BL-A3JM	High Grade	Stage III	T3	M0	N0	1.5849429
TCGA-BL-A5ZZ	High Grade	Stage III	T4a	MX	N0	2.154435019
TCGA-BT-A0S7	High Grade	Stage III	T4a	MX	N0	1.376867593
TCGA-BT-A0YX	High Grade	Stage III	T3b	M0	N0	0.618917068
TCGA-BT-A20J	High Grade	Stage II	T2b	MX	N0	0.924166625
TCGA-BT-A20N	High Grade	Stage III	T3a	MX	N0	0.909699306
TCGA-BT-A20O	High Grade	Stage III	T3a	MX	N0	0.540651663
TCGA-BT-A20P	High Grade	Stage III	T3a	M0	N0	1.174150909
TCGA-BT-A20Q	High Grade	Stage IV	T3b	M0	N2	0.624274877
TCGA-BT-A20R	High Grade	Stage IV	T3b	M0	N1	2.206138918
TCGA-BT-A20T	High Grade	Stage IV	T3b	M0	N1	0.85639506
TCGA-BT-A20U	High Grade	Stage III	T3a	M0	N0	1.520611926
TCGA-BT-A20V	High Grade	Stage IV	T4a	M0	N2	0.63577793
TCGA-BT-A20W	High Grade	Stage II	T2b	M0	N0	0.757821809
TCGA-BT-A20X	High Grade	Stage IV	T4a	M0	N2	1.047349061
TCGA-BT-A2LA	High Grade	Stage III	T3a	M0	N0	0.752603971
TCGA-BT-A2LB	High Grade	Stage III	T3a	M0	N0	0.828332265
TCGA-BT-A2LD	High Grade	Stage IV	T3a	M0	N1	1.174332924
TCGA-BT-A3PH	High Grade	Stage IV	T3b	MX	N2	1.388007925
TCGA-BT-A3PJ	High Grade	Stage III	T3b	M0	N0	0.984632231

TCGA-BT-A3PK	High Grade	Stage II	T2b	MX	N0	1.547997221
TCGA-BT-A42C	High Grade	Stage II	unknow	M0	N0	1.162320698
TCGA-BT-A42E	High Grade	Stage III	T3a	M0	N0	0.956479182
TCGA-BT-A42F	High Grade	Stage IV	T4a	MX	N1	1.017226529
TCGA-C4-A0EZ	High Grade	Stage IV	T3a	M1	N1	1.282433159
TCGA-C4-A0F0	High Grade	Stage II	T2b	M0	N0	0.767125462
TCGA-C4-A0F1	High Grade	Stage III	T3b	M0	N0	1.111381359
TCGA-C4-A0F6	High Grade	Stage III	T3b	M0	N0	1.223449302
TCGA-C4-A0F7	High Grade	Stage IV	T4b	M0	N2	1.130752052
TCGA-CF-A1HR	High Grade	Stage III	T3	M0	N0	0.742577198
TCGA-CF-A1HS	High Grade	Stage III	T3	M0	N0	0.930309859
TCGA-CF-A27C	High Grade	Stage III	T3	M0	N0	0.611498691
TCGA-CF-A3MF	Low Grade	Stage III	T3	M0	N0	0.9458314
TCGA-CF-A3MG	Low Grade	Stage II	T2	M0	N0	0.648283704
TCGA-CF-A3MH	Low Grade	Stage II	T2	M0	N0	0.83744966
TCGA-CF-A3MI	Low Grade	Stage II	T2	M0	N0	1.104596238
TCGA-CF-A47S	Low Grade	Stage II	T2	M0	N0	0.773095847
TCGA-CF-A47T	Low Grade	Stage II	T2	M0	N0	0.717438398
TCGA-CF-A47V	High Grade	Stage II	T2	M0	N0	0.572367299
TCGA-CF-A47W	Low Grade	Stage II	T2	M0	N0	0.960075144
TCGA-CF-A47X	Low Grade	Stage II	T2	M0	N0	0.901035979
TCGA-CF-A47Y	Low Grade	Stage II	T2	M0	N0	0.846935335
TCGA-CF-A5U8	Low Grade	Stage II	T2	M0	N0	0.797548368
TCGA-CF-A5UA	Low Grade	Stage II	T2	M0	N0	0.817855417
TCGA-CF-A7I0	Low Grade	Stage II	T2	M0	N0	0.59020841
TCGA-CF-A8HX	High Grade	Stage II	T2	M0	N0	1.042317161
TCGA-CF-A8HY	High Grade	Stage II	T2	M0	N0	0.427898604
TCGA-CF-A9FF	High Grade	Stage II	T2	M0	N0	0.851489259
TCGA-CF-A9FH	Low Grade	Stage II	T2	M0	N0	0.9729523
TCGA-CF-A9FL	High Grade	Stage III	T3b	M0	N0	1.173754695
TCGA-CF-A9FM	High Grade	Stage I	T1	M0	N0	0.935923951
TCGA-CU-A0YN	High Grade	Stage III	T3a	M0	N0	1.292819062
TCGA-CU-A0YO	High Grade	Stage IV	T3a	MX	N2	0.825692315
TCGA-CU-A0YR	High Grade	Stage IV	T2	M0	N2	1.327869135
TCGA-CU-A3KJ	High Grade	Stage III	T3b	M0	N0	1.025964939
TCGA-CU-A3QU	High Grade	Stage IV	T2b	M0	N1	1.4917178
TCGA-CU-A3YL	High Grade	Stage III	T4a	M0	N0	0.628429154
TCGA-CU-A5W6	High Grade	Stage III	T4a	M0	N0	1.173051197
TCGA-CU-A72E	High Grade	Stage IV	T3b	M0	N2	2.11638503
TCGA-DK-A1A3	High Grade	Stage IV	T3	M0	N2	1.085386267
TCGA-DK-A1A5	High Grade	Stage II	T2b	M0	N0	1.201380131
TCGA-DK-A1A6	High Grade	Stage IV	T2a	M0	N1	0.670788134
TCGA-DK-A1A7	High Grade	Stage IV	T3	M0	N2	0.84351944
TCGA-DK-A1AA	High Grade	Stage III	T3	M0	N0	0.80737665
TCGA-DK-A1AB	High Grade	Stage IV	T4a	M0	N2	1.082053776
TCGA-DK-A1AC	High Grade	Stage III	T3b	M0	N0	0.838568509
TCGA-DK-A1AD	High Grade	Stage IV	T3b	M0	N2	0.702156222
TCGA-DK-A1AE	High Grade	Stage III	T3	M0	N0	0.703502329
TCGA-DK-A1AF	High Grade	Stage IV	T3	M0	N2	1.298542818

TCGA-DK-A1AG	High Grade	Stage III	T3	M0	N0	1.062643607
TCGA-DK-A2HX	High Grade	Stage IV	T3	M0	N2	1.379933744
TCGA-DK-A2I1	High Grade	Stage II	T2b	M0	N0	0.926462747
TCGA-DK-A2I2	High Grade	Stage IV	T3	M0	N3	1.139747961
TCGA-DK-A2I4	High Grade	Stage III	T3b	M0	N0	0.760550789
TCGA-DK-A2I6	High Grade	Stage IV	T2b	M0	N1	0.861164603
TCGA-DK-A3IK	High Grade	Stage IV	T3	M0	N2	1.038248818
TCGA-DK-A3IL	High Grade	Stage IV	T3	M0	N2	1.152782105
TCGA-DK-A3IM	High Grade	Stage III	T3	M0	N0	1.600101863
TCGA-DK-A3IN	High Grade	Stage III	T4a	M0	N0	1.246632921
TCGA-DK-A3IQ	High Grade	Stage III	T3	M0	N0	1.567843006
TCGA-DK-A3IS	High Grade	Stage II	T2a	M0	N0	0.579337969
TCGA-DK-A3IT	High Grade	Stage III	T3	M0	N0	1.131473447
TCGA-DK-A3IU	High Grade	Stage II	T2b	M0	N0	0.802711364
TCGA-DK-A3IV	High Grade	Stage II	unknow	M0	NX	1.015131618
TCGA-DK-A3WW	High Grade	Stage III	T3	M0	N0	0.459724908
TCGA-DK-A3WX	High Grade	Stage III	T3	M0	N0	0.961354643
TCGA-DK-A3WY	High Grade	Stage III	T3	M0	N0	0.833666469
TCGA-DK-A3X1	High Grade	Stage III	T3	M0	N0	1.202480945
TCGA-DK-A3X2	High Grade	Stage IV	T3	M0	N2	1.063841917
TCGA-DK-A6AV	High Grade	Stage II	T2a	M0	N0	0.838596727
TCGA-DK-A6AW	High Grade	Stage II	T2a	M0	N0	0.935804624
TCGA-DK-A6B0	High Grade	Stage II	T2b	M0	N0	1.162264686
TCGA-DK-A6B1	High Grade	Stage II	T2a	M0	N0	0.889151481
TCGA-DK-A6B2	High Grade	Stage IV	T3	M0	N1	1.134015804
TCGA-DK-A6B5	High Grade	Stage IV	T4a	M0	N2	0.96780704
TCGA-DK-A6B6	High Grade	Stage II	unknow	MX	NX	0.778800089
TCGA-DK-AA6L	High Grade	Stage IV	T3	MX	N1	0.785610086
TCGA-DK-AA6M	High Grade	Stage II	T2	M0	N0	0.759543008
TCGA-DK-AA6P	High Grade	Stage II	unknow	M0	N0	1.181616044
TCGA-DK-AA6Q	High Grade	Stage IV	T3	M0	N1	0.389334774
TCGA-DK-AA6R	High Grade	Stage IV	T4	M0	N1	0.800434214
TCGA-DK-AA6S	High Grade	Stage III	T3b	M0	N0	0.913001405
TCGA-DK-AA6T	High Grade	Stage II	unknow	M0	N0	0.78641976
TCGA-DK-AA6U	unknow	Stage II	unknow	M0	N0	0.706216794
TCGA-DK-AA6W	High Grade	Stage II	T2	M0	N0	0.723737718
TCGA-DK-AA6X	High Grade	Stage II	unknow	M0	N0	0.714034746
TCGA-DK-AA71	High Grade	Stage II	T2b	M0	N0	1.048639911
TCGA-DK-AA74	High Grade	Stage III	T3	M0	N0	1.009571244
TCGA-DK-AA75	High Grade	Stage III	T3	M0	N0	0.846130565
TCGA-DK-AA76	High Grade	Stage II	unknow	M0	N0	1.519830855
TCGA-DK-AA77	High Grade	Stage II	T2a	M0	N0	0.615220128
TCGA-E5-A2PC	High Grade	Stage IV	T2b	MX	N1	0.724294941
TCGA-E5-A4TZ	High Grade	Stage IV	T4b	MX	N2	1.741408241
TCGA-E5-A4U1	High Grade	Stage II	T2b	M0	N0	0.718499916
TCGA-E7-A3X6	Low Grade	Stage II	T2	M0	NX	0.624444174
TCGA-E7-A3Y1	Low Grade	Stage II	unknow	M0	N0	0.835411318
TCGA-E7-A4IJ	High Grade	Stage II	T2b	M0	NX	0.651530087
TCGA-E7-A4XJ	High Grade	Stage II	T2	M0	N0	0.678840942

TCGA-E7-A519	High Grade	Stage II	T2b	M0	NX	1.204851555
TCGA-E7-A541	High Grade	Stage II	T2b	MX	N0	0.440074744
TCGA-E7-A5KE	High Grade	Stage II	T2a	M0	N0	1.005201629
TCGA-E7-A5KF	Low Grade	Stage II	T2a	M0	N0	1.248259676
TCGA-E7-A677	Low Grade	Stage II	T2b	M0	N0	0.644464918
TCGA-E7-A678	Low Grade	Stage III	T3	M0	N0	0.844135317
TCGA-E7-A6MD	High Grade	Stage IV	T4a	M0	N1	0.90425732
TCGA-E7-A6ME	High Grade	Stage II	T2b	M0	NX	0.633076844
TCGA-E7-A6MF	Low Grade	Stage II	T2a	M0	NX	0.849166598
TCGA-E7-A7DU	Low Grade	Stage III	T3	M0	N0	1.190603517
TCGA-E7-A7DV	High Grade	Stage IV	T4	MX	N3	1.934552457
TCGA-E7-A7PW	High Grade	Stage III	T3a	M0	NX	0.771003011
TCGA-E7-A7XN	High Grade	Stage III	T3	M0	N0	0.385967856
TCGA-E7-A85H	High Grade	Stage III	T3	M0	N0	0.650632178
TCGA-E7-A8O7	Low Grade	Stage II	T2	M0	N0	0.722357281
TCGA-E7-A8O8	High Grade	Stage II	T2	M0	N0	1.202789494
TCGA-E7-A97P	High Grade	Stage II	T2	M0	NX	0.395550784
TCGA-E7-A97Q	High Grade	Stage IV	T4a	MX	N3	0.964801599
TCGA-FD-A3B3	High Grade	Stage III	T3	MX	N0	0.874463168
TCGA-FD-A3B4	High Grade	Stage III	T4a	MX	N0	1.088979264
TCGA-FD-A3B5	High Grade	Stage IV	T2b	MX	N1	1.398041959
TCGA-FD-A3B6	High Grade	Stage II	T2b	MX	N0	0.839809845
TCGA-FD-A3B7	High Grade	Stage III	T3a	MX	N0	0.728688859
TCGA-FD-A3B8	High Grade	Stage II	T2b	MX	N0	0.94834159
TCGA-FD-A3N5	High Grade	Stage II	T2b	MX	N0	1.196215155
TCGA-FD-A3N6	High Grade	Stage II	T2b	MX	N0	1.078138115
TCGA-FD-A3NA	High Grade	Stage II	T2b	MX	N0	0.727488188
TCGA-FD-A3SJ	High Grade	Stage IV	T2b	MX	N2	1.245523715
TCGA-FD-A3SL	High Grade	Stage IV	T4a	M1	N2	1.509185607
TCGA-FD-A3SM	High Grade	Stage IV	T3a	M1	N2	1.822766355
TCGA-FD-A3SN	High Grade	Stage III	T3b	MX	N0	1.25718352
TCGA-FD-A3SO	High Grade	Stage IV	T3a	MX	N1	1.129797679
TCGA-FD-A3SP	High Grade	Stage III	T3b	MX	N0	1.705977005
TCGA-FD-A3SQ	High Grade	Stage IV	T3a	MX	N2	1.454944065
TCGA-FD-A3SR	High Grade	Stage IV	T4a	MX	N2	0.96798127
TCGA-FD-A3SS	High Grade	Stage IV	T4	MX	N3	0.944311561
TCGA-FD-A43N	High Grade	Stage III	T3a	MX	N0	1.279218166
TCGA-FD-A43P	High Grade	Stage II	T2a	MX	N0	0.632010536
TCGA-FD-A43S	High Grade	Stage III	T3b	MX	N0	0.767262195
TCGA-FD-A43U	High Grade	Stage IV	T4a	MX	N2	1.46915181
TCGA-FD-A43X	High Grade	Stage II	T2a	MX	N0	1.217242477
TCGA-FD-A43Y	High Grade	Stage III	T4	MX	N0	0.963919452
TCGA-FD-A5BR	High Grade	Stage II	T2b	MX	N0	1.005580667
TCGA-FD-A5BS	High Grade	Stage III	T3b	MX	N0	0.757793548
TCGA-FD-A5BT	High Grade	Stage III	T3b	MX	N0	0.893479367
TCGA-FD-A5BU	High Grade	Stage II	T2b	MX	N0	1.008039593
TCGA-FD-A5BV	High Grade	Stage III	T3b	MX	N0	1.436191942
TCGA-FD-A5BX	High Grade	Stage IV	T3b	MX	N1	1.85205457
TCGA-FD-A5BY	High Grade	Stage III	T3a	MX	N0	1.309029323

TCGA-FD-A5BZ	High Grade	Stage IV	T3a	MX	N1	1.755128687
TCGA-FD-A5C0	High Grade	Stage IV	T3a	MX	N2	1.095891959
TCGA-FD-A5C1	High Grade	Stage III	T3b	MX	N0	1.021713519
TCGA-FD-A62N	High Grade	Stage III	T3b	MX	N0	0.642769829
TCGA-FD-A62O	High Grade	Stage IV	T3a	MX	N2	1.259869825
TCGA-FD-A62P	High Grade	Stage II	T2b	MX	N0	0.998562176
TCGA-FD-A62S	High Grade	Stage III	T3b	MX	N0	1.224095677
TCGA-FD-A6TA	High Grade	Stage IV	T3b	MX	N2	1.08666674
TCGA-FD-A6TB	High Grade	Stage III	T3a	MX	N0	0.87264177
TCGA-FD-A6TC	High Grade	Stage III	T4a	MX	N0	1.741596667
TCGA-FD-A6TD	High Grade	Stage III	T3a	MX	N0	1.338663257
TCGA-FD-A6TE	High Grade	Stage IV	T3a	MX	N2	0.891693941
TCGA-FD-A6TF	High Grade	Stage IV	T3b	M1	N2	1.313198879
TCGA-FD-A6TG	High Grade	Stage IV	T3a	MX	N2	1.152881999
TCGA-FD-A6TH	High Grade	Stage IV	T3	MX	N2	1.644298057
TCGA-FD-A6TI	High Grade	Stage IV	T4b	MX	N1	0.930193562
TCGA-FD-A6TK	High Grade	Stage III	T3a	MX	N0	0.808269566
TCGA-FJ-A3Z7	High Grade	Stage IV	T4a	MX	N2	0.903249141
TCGA-FJ-A3Z9	High Grade	unknow	TX	M0	N0	1.183134147
TCGA-FJ-A3ZE	High Grade	Stage IV	unknow	M1	N3	1.012859176
TCGA-FJ-A3ZF	High Grade	Stage III	unknow	M0	N0	0.879719556
TCGA-FJ-A871	High Grade	Stage III	T3b	MX	NX	0.776577887
TCGA-FT-A3EE	High Grade	Stage III	T4a	MX	N0	1.099587812
TCGA-FT-A61P	High Grade	Stage IV	T3b	MX	N2	1.438958799
TCGA-G2-A2EC	High Grade	Stage II	unknow	M0	N0	0.907465302
TCGA-G2-A2EF	High Grade	Stage II	unknow	M0	N0	0.58754059
TCGA-G2-A2EJ	High Grade	Stage II	unknow	M0	N0	1.301422809
TCGA-G2-A2EK	High Grade	Stage II	unknow	M0	N0	0.928467318
TCGA-G2-A2EL	High Grade	Stage II	unknow	M0	N0	0.824410069
TCGA-G2-A2EO	High Grade	Stage III	T3a	M0	N0	0.663275705
TCGA-G2-A2ES	High Grade	Stage II	T3b	M0	N0	1.080248652
TCGA-G2-A3IB	High Grade	Stage II	unknow	MX	NX	1.509557616
TCGA-G2-A3IE	High Grade	Stage II	unknow	MX	NX	1.249271111
TCGA-G2-A3VY	High Grade	Stage II	unknow	unknow	unknow	0.713778807
TCGA-G2-AA3B	High Grade	Stage II	T2	M0	N0	0.547403516
TCGA-G2-AA3C	High Grade	Stage IV	T3b	M0	N1	1.827791884
TCGA-G2-AA3D	High Grade	Stage IV	T3	M0	N2	0.90097348
TCGA-G2-AA3F	High Grade	Stage IV	T3	M0	N1	1.507839512
TCGA-GC-A3BM	High Grade	Stage II	T2b	M0	N0	0.715975632
TCGA-GC-A3I6	High Grade	Stage III	T3a	M0	N0	1.242766416
TCGA-GC-A3OO	High Grade	Stage II	T2b	M0	N0	1.881259668
TCGA-GC-A3RB	High Grade	Stage III	T3b	M0	N0	0.61769371
TCGA-GC-A3RC	High Grade	Stage II	T2b	M0	N0	1.726686597
TCGA-GC-A3RD	High Grade	Stage III	T3a	M0	N0	1.812135759
TCGA-GC-A3WC	High Grade	Stage III	T3	MX	N0	0.699160685
TCGA-GC-A3YS	High Grade	Stage IV	T3a	MX	N1	1.390753987
TCGA-GC-A4ZW	High Grade	Stage III	T3a	M0	N0	0.750718772
TCGA-GC-A6I1	High Grade	Stage II	T2b	MX	N0	1.118946029
TCGA-GC-A6I3	High Grade	Stage IV	T3a	MX	N1	0.986437809
TCGA-GD-A2C5	High Grade	Stage IV	T3a	MX	N2	1.106636506

TCGA-GD-A3OP	High Grade	Stage IV	T4a	MX	N2	0.838714133
TCGA-GD-A3OQ	High Grade	Stage IV	T4a	MX	N1	1.408783835
TCGA-GD-A3OS	High Grade	Stage II	unknow	MX	NX	1.503834564
TCGA-GD-A6C6	High Grade	Stage III	T3a	MX	N0	1.869833664
TCGA-GD-A76B	High Grade	Stage II	T2b	MX	N0	0.693656916
TCGA-GU-A42P	High Grade	Stage IV	T3a	M0	N1	1.106444097
TCGA-GU-A42Q	High Grade	Stage III	T3b	M0	N0	1.199746734
TCGA-GU-A42R	High Grade	Stage IV	T4a	MX	N2	0.990280721
TCGA-GU-A762	High Grade	Stage IV	T4a	MX	N2	0.615278909
TCGA-GU-A763	High Grade	Stage III	T4	M0	N0	0.685010239
TCGA-GU-A764	High Grade	Stage II	T2b	MX	N0	0.898128998
TCGA-GU-A766	High Grade	Stage II	T2a	MX	N0	0.587182492
TCGA-GU-A767	High Grade	Stage IV	T3b	MX	N2	1.059341377
TCGA-GU-AATO	High Grade	Stage IV	T4a	MX	N2	0.915643036
TCGA-GU-AATP	High Grade	Stage IV	T2	MX	N2	1.686033888
TCGA-GU-AATQ	High Grade	Stage III	T3b	MX	N0	1.562223742
TCGA-GV-A3JV	High Grade	Stage IV	T3b	MX	N1	0.695989382
TCGA-GV-A3JW	High Grade	Stage II	T2	MX	NX	1.268146203
TCGA-GV-A3JX	High Grade	Stage III	T3b	MX	N0	0.936105905
TCGA-GV-A3JZ	High Grade	Stage IV	T4a	MX	N3	1.252424571
TCGA-GV-A3QF	High Grade	Stage IV	T3b	MX	N2	1.077134768
TCGA-GV-A3QG	High Grade	Stage IV	T3a	MX	N3	1.015234928
TCGA-GV-A3QH	High Grade	Stage II	unknow	MX	NX	1.407477985
TCGA-GV-A3QI	High Grade	Stage III	T3b	MX	N0	1.358743827
TCGA-GV-A3QK	High Grade	Stage IV	T4a	M0	N2	0.726598883
TCGA-GV-A40E	High Grade	Stage II	unknow	MX	NX	1.011824494
TCGA-GV-A40G	High Grade	Stage II	T2a	MX	N0	0.978603261
TCGA-GV-A6ZA	High Grade	Stage II	T2b	MX	N0	0.711659964
TCGA-H4-A2HO	High Grade	Stage III	T4a	MX	N0	1.118448825
TCGA-H4-A2HQ	High Grade	Stage IV	unknow	M1	NX	0.814412843
TCGA-HQ-A2OE	unknow	unknow	T2a	MX	N2	0.597573718
TCGA-HQ-A2OF	High Grade	Stage III	T3b	M0	N0	0.894051272
TCGA-HQ-A5ND	High Grade	Stage IV	T3b	M0	N1	0.659371172
TCGA-HQ-A5NE	High Grade	Stage III	T3	M0	N0	1.363093809
TCGA-K4-A3WS	High Grade	Stage III	T3a	MX	N0	0.958902751
TCGA-K4-A3WU	High Grade	Stage III	T4a	MX	N0	0.97294953
TCGA-K4-A3WV	High Grade	Stage II	T2b	MX	N0	1.161825872
TCGA-K4-A4AB	High Grade	Stage III	T4a	MX	N0	0.952780664
TCGA-K4-A4AC	High Grade	Stage II	T2b	MX	N0	1.406488567
TCGA-K4-A54R	High Grade	Stage II	T2b	MX	N0	0.674971527
TCGA-K4-A5RH	High Grade	Stage III	T3a	MX	N0	0.493961984
TCGA-K4-A5RI	High Grade	Stage III	T3a	MX	N0	0.756091417
TCGA-K4-A5RJ	High Grade	Stage II	T2b	MX	N0	0.69032809
TCGA-K4-A6FZ	High Grade	Stage III	T3a	MX	N0	1.24479469
TCGA-K4-A6MB	High Grade	Stage IV	T3b	MX	N1	2.316122838
TCGA-K4-A83P	unknow	Stage IV	T4a	MX	N1	0.955394184
TCGA-K4-AAQO	High Grade	Stage III	T3a	MX	N0	1.017955888
TCGA-KQ-A41N	High Grade	Stage III	T3b	M0	N0	1.191933021
TCGA-KQ-A41O	High Grade	Stage IV	T3	M0	N1	0.475145799

TCGA-KQ-A41P	High Grade	Stage IV	T3b	M1	N3	2.619136186
TCGA-KQ-A41Q	High Grade	Stage III	T3b	MX	N0	1.411536582
TCGA-KQ-A41R	High Grade	Stage II	T2	MX	N0	1.563756224
TCGA-KQ-A41S	High Grade	Stage III	T4a	MX	NX	1.467644033
TCGA-LC-A66R	High Grade	Stage IV	T4a	MX	N2	0.792883134
TCGA-LT-A5Z6	High Grade	Stage II	unknow	MX	NX	0.907603741
TCGA-LT-A8JT	High Grade	Stage II	T2a	M0	N0	0.765026867
TCGA-MV-A51V	High Grade	Stage III	T3a	M0	N0	1.061919807
TCGA-PQ-A6FI	High Grade	Stage II	T2a	MX	N0	0.847797336
TCGA-PQ-A6FN	High Grade	Stage III	T3a	MX	N0	1.32148547
TCGA-R3-A69X	High Grade	Stage III	T3a	M0	N0	0.85455038
TCGA-S5-A6DX	High Grade	Stage IV	T4a	MX	N2	1.014034227
TCGA-S5-AA26	High Grade	Stage III	T3a	MX	N0	1.235182271
TCGA-SY-A9G0	High Grade	Stage IV	T4	M0	N1	1.182721861
TCGA-SY-A9G5	High Grade	Stage III	T4a	M0	N0	1.081389756
TCGA-UY-A78K	High Grade	Stage IV	unknow	MX	N2	0.961848133
TCGA-UY-A78L	High Grade	Stage IV	unknow	MX	N1	1.735641345
TCGA-UY-A78M	High Grade	Stage IV	T2	MX	N2	1.559880122
TCGA-UY-A78N	High Grade	Stage IV	T2	MX	N1	0.791391029
TCGA-UY-A78O	High Grade	Stage II	T2	MX	N0	1.312061023
TCGA-UY-A78P	High Grade	Stage II	T2	MX	N0	1.544931628
TCGA-UY-A8OB	High Grade	Stage IV	T3a	MX	N1	0.666020158
TCGA-UY-A8OC	High Grade	Stage IV	T4	MX	N1	2.072535324
TCGA-UY-A8OD	High Grade	Stage II	T2b	MX	N0	1.311412354
TCGA-UY-A9PA	High Grade	Stage III	T3a	MX	N0	0.676893736
TCGA-UY-A9PB	High Grade	Stage III	T3a	MX	N0	1.010131217
TCGA-UY-A9PD	High Grade	Stage III	T3a	MX	N0	1.620069459
TCGA-UY-A9PE	High Grade	Stage IV	T2b	MX	N2	1.306549592
TCGA-UY-A9PF	High Grade	Stage IV	T3a	MX	N2	0.96734319
TCGA-UY-A9PH	High Grade	Stage II	T2b	MX	N0	0.783951422
TCGA-XF-A8HB	High Grade	Stage II	T2b	MX	N0	1.274536701
TCGA-XF-A8HC	High Grade	Stage IV	T3a	MX	N2	1.221966404
TCGA-XF-A8HD	High Grade	Stage III	T3a	MX	N0	0.621032344
TCGA-XF-A8HE	High Grade	Stage III	T3b	MX	N0	0.726366312
TCGA-XF-A8HF	High Grade	Stage III	T3a	M0	N0	1.467242221
TCGA-XF-A8HG	High Grade	Stage III	T3b	MX	N0	1.09674257
TCGA-XF-A8HH	High Grade	Stage IV	T3b	M0	N2	1.328158025
TCGA-XF-A8HI	High Grade	Stage IV	T2b	MX	N2	0.980630975
TCGA-XF-A9SH	High Grade	Stage II	T2b	M0	N0	1.162833233
TCGA-XF-A9SI	High Grade	Stage II	T2b	MX	N0	0.613459032
TCGA-XF-A9SJ	High Grade	Stage IV	T3b	MX	N2	0.798876693
TCGA-XF-A9SK	High Grade	Stage IV	T3b	MX	N1	1.135907142
TCGA-XF-A9SL	High Grade	Stage IV	T3a	MX	N2	0.920334881
TCGA-XF-A9SM	High Grade	Stage III	T3b	MX	N0	0.739135402
TCGA-XF-A9SP	High Grade	Stage III	T3b	MX	N0	1.123826159
TCGA-XF-A9ST	High Grade	Stage III	T3b	MX	N0	1.098052279
TCGA-XF-A9SU	High Grade	Stage IV	T3b	MX	N1	1.126319807
TCGA-XF-A9SV	High Grade	Stage IV	T4a	M1	N2	1.917543259
TCGA-XF-A9SW	High Grade	Stage IV	T3b	MX	N2	1.524534485

TCGA-XF-A9SX	High Grade	Stage IV	T3b	MX	N2	1.058807283
TCGA-XF-A9SY	High Grade	Stage IV	T3b	MX	N2	1.135546594
TCGA-XF-A9SZ	High Grade	Stage IV	T3b	MX	N2	2.22660383
TCGA-XF-A9T0	High Grade	Stage III	T3b	MX	N0	1.056622031
TCGA-XF-A9T2	High Grade	Stage III	T3b	MX	N0	1.755874823
TCGA-XF-A9T3	High Grade	Stage IV	T3b	MX	N2	1.506401754
TCGA-XF-A9T4	High Grade	Stage IV	T2b	MX	N1	0.999906518
TCGA-XF-A9T5	High Grade	Stage IV	T3a	MX	N1	0.705576606
TCGA-XF-A9T6	High Grade	Stage III	T3b	MX	N0	1.158525835
TCGA-XF-A9T8	High Grade	Stage III	T3b	MX	N0	0.854784264
TCGA-XF-AAME	High Grade	Stage II	T2b	MX	N0	1.360455702
TCGA-XF-AAMG	High Grade	Stage III	T4a	MX	N0	1.569581878
TCGA-XF-AAMH	High Grade	Stage IV	T3b	MX	N1	1.255741481
TCGA-XF-AAMJ	High Grade	Stage III	T3b	M0	N0	1.31307036
TCGA-XF-AAML	High Grade	Stage II	T2b	MX	N0	0.608299673
TCGA-XF-AAMQ	High Grade	Stage II	T2a	MX	N0	0.934158679
TCGA-XF-AAMR	High Grade	Stage III	T3b	MX	N0	1.358318356
TCGA-XF-AAMT	High Grade	Stage IV	T3b	MX	N2	2.218765796
TCGA-XF-AAMW	High Grade	Stage IV	T2b	unknow	N0	1.172824504
TCGA-XF-AAMX	High Grade	Stage III	T3b	MX	N0	1.782543669
TCGA-XF-AAMY	High Grade	Stage III	T3b	MX	N0	1.78167895
TCGA-XF-AAMZ	High Grade	Stage IV	T3a	MX	N2	1.250240673
TCGA-XF-AAN0	High Grade	Stage IV	T4a	M0	N2	0.885798205
TCGA-XF-AAN1	High Grade	Stage III	T4a	M0	N0	0.448902309
TCGA-XF-AAN2	High Grade	Stage II	T2b	MX	N0	0.886458845
TCGA-XF-AAN3	High Grade	Stage IV	T3b	MX	N2	0.860432569
TCGA-XF-AAN4	High Grade	Stage III	T3b	MX	N0	1.033693552
TCGA-XF-AAN5	High Grade	Stage III	T3b	MX	N0	0.792577285
TCGA-XF-AAN7	High Grade	Stage IV	T3a	MX	N1	1.599068294
TCGA-XF-AAN8	High Grade	Stage III	T3b	MX	N0	1.425122564
TCGA-YC-A89H	High Grade	Stage II	unknow	MX	unknow	1.639017046
TCGA-YC-A8S6	High Grade	Stage II	T2a	MX	N0	0.927276807
TCGA-YC-A9TC	High Grade	Stage IV	unknow	M1	unknow	1.227564153
TCGA-YF-AA3L	High Grade	Stage II	T2b	MX	N0	0.795565382
TCGA-YF-AA3M	High Grade	Stage II	T2a	MX	NX	1.166593454
TCGA-ZF-A9R0	High Grade	Stage III	T3b	M0	NX	1.085338807
TCGA-ZF-A9R1	High Grade	Stage IV	T3b	M0	N1	0.920624087
TCGA-ZF-A9R2	High Grade	Stage II	T2b	M0	N0	0.87947563
TCGA-ZF-A9R3	High Grade	Stage II	T2	M0	NX	0.653086167
TCGA-ZF-A9R4	High Grade	Stage II	T2	M0	NX	0.747147841
TCGA-ZF-A9R5	High Grade	Stage III	T3	M0	N0	0.760913823
TCGA-ZF-A9R7	High Grade	Stage II	unknow	M0	NX	0.462957881
TCGA-ZF-A9R9	High Grade	Stage IV	T3b	MX	N2	1.143688686
TCGA-ZF-A9RC	High Grade	Stage III	T3a	MX	N0	1.532364675
TCGA-ZF-A9RD	High Grade	Stage IV	T3a	MX	N2	0.722850348
TCGA-ZF-A9RE	High Grade	Stage II	unknow	MX	unknow	0.933158116
TCGA-ZF-A9RF	High Grade	Stage II	T1	M0	NX	0.622829224
TCGA-ZF-A9RL	High Grade	Stage II	unknow	MX	unknow	0.492544953
TCGA-ZF-A9RM	High Grade	Stage II	T0	MX	N0	0.824019602

TCGA-ZF-A9RN	High Grade	Stage III	T3b	M0	NX	0.553121931
TCGA-ZF-AA4N	High Grade	Stage II	unknow	unknow	unknow	0.532726758
TCGA-ZF-AA4R	High Grade	Stage IV	T3a	MX	N1	1.44205472
TCGA-ZF-AA4T	High Grade	Stage IV	T4	MX	N2	1.272606743
TCGA-ZF-AA4U	High Grade	Stage III	T4a	MX	NX	0.629454894
TCGA-ZF-AA4V	High Grade	Stage III	T3b	M0	N0	0.70943908
TCGA-ZF-AA4W	High Grade	Stage III	T3b	MX	N0	1.077334552
TCGA-ZF-AA4X	High Grade	Stage II	T2	M0	NX	1.081171073
TCGA-ZF-AA51	High Grade	Stage II	T2	M0	NX	1.101289942
TCGA-ZF-AA52	High Grade	Stage III	T3a	MX	NX	1.759942408
TCGA-ZF-AA53	High Grade	Stage II	T2	M0	NX	1.053384694
TCGA-ZF-AA54	High Grade	Stage III	T3	MX	NX	2.37311043
TCGA-ZF-AA56	High Grade	Stage III	T4a	MX	N0	1.039202586
TCGA-ZF-AA58	High Grade	Stage IV	T3a	MX	N2	1.477814046
TCGA-ZF-AA5H	High Grade	Stage IV	T3b	M0	N2	1.289620157
TCGA-ZF-AA5N	High Grade	Stage IV	T2	M1	NX	1.010082031
TCGA-ZF-AA5P	High Grade	Stage IV	T2b	M0	N2	0.732294781

Table S4. Differentially expressed genes between high TIICs and low TIICs levels

gene	conMean	treatMean	logFC	*p*Value	FDR
KLRK1	32.29593089	15.56723899	-1.052839314	3.43E-12	4.29E-08
RP5-907D15.4	18.99831074	41.40795535	1.124036822	3.36E-12	4.29E-08
COL5A3	1103.436623	2277.066039	1.045172364	4.90E-11	2.69E-07
LINC01561	8.206788473	20.19896124	1.299391428	5.37E-11	2.69E-07
COL1A1	116635.661	264848.9818	1.183161007	1.10E-10	3.45E-07
RP11-863P13.3	24.3341532	61.67945799	1.341807516	1.75E-10	4.72E-07
TRAV19	14.32655382	6.89025777	-1.056061757	1.88E-10	4.72E-07
ADAMTS12	474.3262996	1129.665525	1.25194391	3.73E-10	7.18E-07
SSC5D	426.9124064	924.5654147	1.114835308	5.66E-10	9.40E-07
OLFML2B	1059.990556	2144.305005	1.016458717	6.00E-10	9.40E-07
CD8A	802.4900871	254.1721513	-1.658677603	6.64E-10	9.79E-07
COL1A2	68375.63982	151753.763	1.150177958	7.71E-10	1.07E-06
PLPP4	131.4300883	294.586665	1.164396536	8.57E-10	1.07E-06
TRGC2	63.93936597	20.25124568	-1.658693785	1.06E-09	1.27E-06
MXRA8	2513.510805	5080.568618	1.015286081	1.14E-09	1.30E-06
RP11-394I13.1	4.119454085	9.990277726	1.278071623	1.55E-09	1.50E-06
AC092580.4	56.24211134	20.9779139	-1.422779535	1.52E-09	1.50E-06
P4HA3	170.1538612	353.4361184	1.05460959	1.93E-09	1.66E-06
RP11-400N13.3	9.019124975	27.71194429	1.619448558	2.90E-09	1.79E-06
TRGV10	10.57401326	3.664886321	-1.528682687	2.59E-09	1.79E-06
COL3A1	66408.85403	154121.3681	1.214619389	2.26E-09	1.79E-06
RPLP0P2	118.5931049	259.6476289	1.130534918	2.89E-09	1.79E-06
COL10A1	654.8048683	1807.923625	1.46519678	2.69E-09	1.79E-06
CTD-2171N6.1	9.988971838	45.78115512	2.19634577	2.85E-09	1.79E-06
POSTN	6764.077048	14983.54966	1.147414446	3.51E-09	2.09E-06
MMP9	1432.237847	11158.99787	2.96186447	3.71E-09	2.16E-06
ZNF469	368.9656911	808.0845354	1.131019553	4.13E-09	2.22E-06
MMP8	3.207257991	9.600385433	1.581751919	4.42E-09	2.22E-06

PCOLCE	2295.854539	4679.91945	1.02745246	4.37E-09	2.22E-06
MMP11	5115.514815	12688.86495	1.31061168	4.88E-09	2.31E-06
FASLG	61.94279933	22.35883866	-1.470091328	6.84E-09	2.90E-06
RP11-426C22.4	16.04008513	34.2838163	1.095845913	6.75E-09	2.90E-06
FNDC1	638.2170105	1380.973298	1.113566458	7.12E-09	2.90E-06
RP11-290O12.2	2.461657973	5.625817251	1.192432364	7.19E-09	2.90E-06
COL6A3	16799.58612	34760.23375	1.049012093	7.86E-09	3.08E-06
ITGA11	814.113355	2255.520544	1.470158836	1.13E-08	4.10E-06
THEMIS	68.87020467	28.16087902	-1.290187597	1.30E-08	4.57E-06
RP11-366L20.2	15.59782618	37.65763871	1.271597561	1.63E-08	5.52E-06
ASPN	517.4808505	1440.542895	1.477035239	1.69E-08	5.64E-06
CD3D	448.0191748	196.3428903	-1.190185122	1.85E-08	6.03E-06
TTC24	17.69579587	7.284749549	-1.28045537	2.05E-08	6.49E-06
AEBP1	9883.126567	19834.35197	1.004961841	2.08E-08	6.52E-06
RP11-291B21.2	93.11495982	22.68943647	-2.036992192	2.36E-08	7.20E-06
SGCD	151.7796412	340.2482043	1.164609259	2.97E-08	8.60E-06
SFRP2	3603.07909	9209.44311	1.3538836	2.96E-08	8.60E-06
RP11-429E11.2	1.531435953	3.6940098	1.270302661	4.07E-08	1.06E-05
GPR171	90.90879142	40.00907397	-1.184092581	4.97E-08	1.23E-05
GPR25	14.03748867	5.21923363	-1.427374969	5.06E-08	1.24E-05
CLEC11A	513.8637962	1096.243646	1.093110563	5.19E-08	1.25E-05
LINC01614	35.52626212	93.62240817	1.397967971	5.49E-08	1.30E-05
TRAV12-1	7.592845511	2.839784308	-1.418859298	5.98E-08	1.35E-05
SIRPG	201.2725569	76.58831229	-1.393954325	6.34E-08	1.42E-05
GZMH	284.6870218	81.91377169	-1.797198796	6.88E-08	1.51E-05
ADGRG5	162.4927559	65.67492802	-1.306960783	7.31E-08	1.58E-05
RP1-47M23.3	10.49201909	4.301958297	-1.286226893	7.39E-08	1.58E-05
NID2	445.401448	907.0150475	1.026020237	9.26E-08	1.81E-05
KLRC1	73.10917682	20.50920684	-1.833780809	9.44E-08	1.82E-05
CD3G	182.6167066	82.61618202	-1.144322461	1.45E-07	2.47E-05
UBD	736.2640348	246.8009608	-1.576875219	1.52E-07	2.53E-05
BNC2	209.7139535	425.8661757	1.021977293	1.53E-07	2.53E-05
ADGRF2	10.66512392	30.81285576	1.53063167	1.90E-07	3.09E-05
ISLR	2317.875847	5431.82779	1.228634448	1.94E-07	3.14E-05
TBX21	75.53591554	29.84094232	-1.339869681	2.10E-07	3.35E-05
FAM180A	23.96389903	58.90150238	1.297441773	2.14E-07	3.37E-05
IFNG	56.68548541	14.14297392	-2.002893858	2.18E-07	3.41E-05
TRAT1	50.8565739	18.22224331	-1.480733696	2.25E-07	3.47E-05
FLJ16779	14.90151878	38.23763805	1.359534031	2.28E-07	3.49E-05
KLRC4-KLRK1	6.885943995	3.378009455	-1.027481081	2.28E-07	3.49E-05
FAM69C	7.755327468	23.16496229	1.578684728	2.34E-07	3.53E-05
LUM	10416.11364	20947.8185	1.007982916	2.41E-07	3.62E-05
UNC5C	103.1888479	227.4415689	1.140208895	2.58E-07	3.68E-05
RP4-598P13.1	1.547237825	4.551724219	1.55671818	2.59E-07	3.68E-05
FIBIN	182.0286089	464.5127728	1.351553055	2.52E-07	3.68E-05
ZNF683	232.1043518	63.9828018	-1.859017498	2.51E-07	3.68E-05
CAMK2A	20.21070305	41.44129258	1.035949494	2.62E-07	3.69E-05
GPR1	53.56019324	145.9564143	1.446304543	2.87E-07	3.95E-05
LRRC15	534.0061225	1241.744298	1.217439934	3.11E-07	4.19E-05

CTSK	2759.266808	6500.287204	1.236218498	3.14E-07	4.21E-05
PRRG3	14.4870764	40.60704763	1.486963661	3.18E-07	4.23E-05
RP11-893F2.6	0.78373929	1.733027911	1.144849162	3.21E-07	4.26E-05
SCML4	59.17734511	25.76994061	-1.199355761	3.34E-07	4.38E-05
ADAMTS16	111.9881459	228.5702782	1.029291788	3.81E-07	4.75E-05
TRBV27	4.730181132	1.735875591	-1.446231875	3.86E-07	4.79E-05
COL11A1	965.6033333	2809.145059	1.540628563	4.15E-07	5.00E-05
CIITA	1695.976141	826.5330469	-1.036971466	4.24E-07	5.09E-05
TRDV1	9.157231905	2.018720197	-2.181470598	4.99E-07	5.73E-05
RP11-184M15.1	2.358725851	8.182811789	1.794588922	5.04E-07	5.77E-05
KLHL4	24.72450938	59.23133769	1.260418775	5.40E-07	6.12E-05
HS3ST2	36.42882585	78.83428829	1.113742758	5.64E-07	6.23E-05
KLK4	35.1069741	101.30505	1.528876535	5.80E-07	6.34E-05
CD2	694.883988	324.0992819	-1.100336314	6.13E-07	6.56E-05
MCHR1	18.14927729	37.01088382	1.028037487	6.37E-07	6.73E-05
SLA2	179.2393765	80.1056057	-1.161912504	6.35E-07	6.73E-05
TSSC2	23.73008145	51.99499577	1.131655726	6.51E-07	6.83E-05
TNN	27.40980415	170.1419839	2.633975257	6.71E-07	6.98E-05
OBP2A	3.293382609	8.637736997	1.391083263	6.94E-07	7.12E-05
HILS1	1.320924977	3.151618536	1.254544396	7.16E-07	7.15E-05
CD3E	917.042454	405.9464278	-1.175699175	7.16E-07	7.15E-05
RPSAP52	19.58778261	49.46283896	1.336390957	7.50E-07	7.39E-05
ZNF831	66.01141657	29.05053843	-1.184150655	8.69E-07	8.31E-05
AC112721.1	7.628346993	24.04686541	1.656406472	8.77E-07	8.31E-05
RP11-13P5.2	6.010607827	12.32441353	1.035936199	8.79E-07	8.31E-05
RP11-417E7.2	16.95527358	34.71222584	1.033709815	9.46E-07	8.84E-05
KLRC4	3.741373627	1.686132519	-1.149850119	9.74E-07	9.01E-05
TM4SF19	57.95204343	128.8637456	1.152914997	1.01E-06	9.20E-05
UBASH3A	90.37645268	41.14305887	-1.135297873	1.02E-06	9.21E-05
CHI3L1	2199.549175	7891.36789	1.843067543	1.04E-06	9.27E-05
DIRC1	3.443847402	7.480459101	1.119105598	1.06E-06	9.31E-05
PRND	13.88009299	67.73959351	2.286982096	1.06E-06	9.31E-05
CXCR2P1	111.9852047	41.58018965	-1.429339894	1.32E-06	0.000108355
KIR2DL4	51.52091684	18.20838173	-1.500555559	1.32E-06	0.000108393
CSDC2	124.6258342	264.907375	1.087884847	1.33E-06	0.000108562
ATP6V0D2	18.53150563	71.80065381	1.95401688	1.34E-06	0.000109124
IL36RN	125.8206148	419.2238974	1.736352642	1.44E-06	0.000114847
OR2I1P	511.5906276	149.897202	-1.77101638	2.05E-06	0.000154214
IGFL3	11.263452	28.65134763	1.346953948	2.12E-06	0.000157033
RP11-356O9.2	58.60751196	28.66435376	-1.031827839	2.42E-06	0.00017235
TRIML2	25.78885412	57.75101935	1.16309874	2.43E-06	0.000172956
TRBV4-1	8.805433288	3.114088019	-1.499584274	2.59E-06	0.000180319
LCK	631.009647	308.1136576	-1.034199428	2.67E-06	0.00018254
SFRP4	2087.250529	4609.983158	1.143157705	2.86E-06	0.000189509
KERA	1.752572673	5.913147461	1.754451986	2.86E-06	0.000189509
LINC00656	1.765659185	4.533529315	1.360427719	3.15E-06	0.000203087
TMEM132B	18.11600975	37.93528212	1.066275046	3.18E-06	0.000204269
GIP	1.787787903	3.845374164	1.104948393	3.26E-06	0.000208836
GPR174	20.85671604	8.41880979	-1.308823826	3.55E-06	0.000222552

RTP5	7.724542781	2.187044098	-1.820467232	3.59E-06	0.000224246
SH2D1A	126.869246	53.1837082	-1.254286115	3.62E-06	0.000225721
RP11-1094M14.5	11.96139358	5.21351319	-1.1980577	3.83E-06	0.000235075
NKAIN4	19.05228511	47.2896274	1.311559731	3.90E-06	0.000237476
CLSTN2	140.7534379	349.1948616	1.310862169	3.94E-06	0.000239791
PDCD1	185.1676458	67.115826	-1.464107139	4.28E-06	0.000255605
MFAP5	415.8417197	892.2143357	1.101355824	4.55E-06	0.000269477
RP11-1094M14.8	41.63182295	19.47522086	-1.096047042	4.58E-06	0.000269833
FGFR1	1323.723519	3029.877203	1.194657501	4.67E-06	0.000272738
JAKMIP1	72.55779522	31.29072215	-1.213395664	4.82E-06	0.000279671
IL21-AS1	15.30996822	6.399462521	-1.258448642	4.98E-06	0.000284856
ZCCHC5	1.803907212	4.978748377	1.464657972	5.08E-06	0.000289364
CST6	956.5678384	2213.249432	1.21022686	5.44E-06	0.000304056
MAP4K1	540.0690153	239.4890483	-1.173184097	5.50E-06	0.000307029
ABCB5	3.769642223	9.529490136	1.337971423	5.60E-06	0.000310298
SPTLC1P4	0.910343325	2.045332425	1.167852693	5.71E-06	0.000313553
PYHIN1	104.0318907	42.95878985	-1.276000593	5.77E-06	0.000314355
RETN	7.302585741	14.98522639	1.037061583	5.90E-06	0.000319169
LINC00426	55.07337202	23.69033765	-1.217056183	5.94E-06	0.00031975
LIPN	2.969515964	11.96754689	2.010827765	5.96E-06	0.000320443
TRIM63	28.05116162	56.60258587	1.012807449	6.33E-06	0.000334532
LRRN4	14.70981396	34.60744925	1.23430361	6.55E-06	0.000343411
RP11-260M19.2	0.617037494	1.555614158	1.334054208	6.82E-06	0.000352028
FAM196B	3.480870248	8.5817728	1.301827669	6.95E-06	0.000355324
OMD	33.72750728	86.41847203	1.357414027	7.22E-06	0.000365188
LILRP2	9.053111229	3.508661467	-1.367492924	8.06E-06	0.000399768
SCUBE1	111.46256	53.46848464	-1.059798499	8.08E-06	0.000399768
TRGC1	23.658518	9.858777634	-1.262879018	8.17E-06	0.00040349
NKG7	689.2681133	252.5984542	-1.448219465	8.37E-06	0.000407667
TRAV17	8.945809966	4.08688577	-1.130210192	8.86E-06	0.000428329
KEL	158.0446464	57.20843421	-1.466032403	8.89E-06	0.000428954
KLHDC8A	25.31579107	71.30994591	1.494065743	9.08E-06	0.000433254
TRAV21	10.33054044	3.944008054	-1.389181328	9.20E-06	0.000437412
LINC01429	2.506882145	5.111407874	1.027826546	9.91E-06	0.000464641
LINC01449	0.595331292	1.390768443	1.224117604	1.02E-05	0.000473988
AC104820.2	9.374374485	3.840228528	-1.287530261	1.06E-05	0.000485382
RP3-495K2.2	1.169653643	2.675562353	1.193760768	1.12E-05	0.000509765
TSKS	21.68963571	58.49325014	1.431264331	1.13E-05	0.000511131
CXCR3	168.4639138	68.98085199	-1.288171735	1.16E-05	0.000522335
ITK	238.5400056	112.9060254	-1.079108761	1.22E-05	0.000546368
LINC01048	1.19911198	2.456418941	1.03459024	1.36E-05	0.000586217
TRAV12-2	13.57858253	5.877141652	-1.208146308	1.38E-05	0.000594209
RP11-567M16.1	4.956315525	10.81657979	1.12590445	1.39E-05	0.00059638
LINC01050	2.746790546	6.624399857	1.270042855	1.39E-05	0.00059688
COL6A6	20.66324326	44.37168425	1.102572601	1.41E-05	0.000604863
KLKP1	0.944275876	4.735250557	2.326160446	1.46E-05	0.00062114
FTH1P22	12.23580045	5.252223588	-1.220108245	1.49E-05	0.000630802
CYTL1	49.10607317	114.4465406	1.220700489	1.49E-05	0.000630802
GZMB	1092.02488	299.7673136	-1.86509074	1.50E-05	0.00063456

AL359753.1	3.344820721	1.342325412	-1.317194428	1.54E-05	0.000646804
CTC-303L1.1	3.514502452	1.624640021	-1.113200372	1.56E-05	0.000652266
SIRPG-AS1	2.669293006	0.984207431	-1.439423363	1.60E-05	0.000663284
IDO2	17.13422528	5.619572573	-1.608348654	1.61E-05	0.000665369
RP11-109E24.1	2.752395519	0.808904576	-1.766646373	1.63E-05	0.000670851
COLEC12	420.1006842	874.5704393	1.05783945	1.67E-05	0.000683959
AHNAK2	2299.427379	5644.872088	1.295666255	1.72E-05	0.000697794
TRBV7-6	5.661927829	2.268682432	-1.319438684	1.73E-05	0.000700942
TRBC1	21.04839958	10.34262539	-1.025108094	1.78E-05	0.000713665
ADRA1B	14.66595996	35.24700764	1.265029276	1.83E-05	0.000728776
KLF17	5.878758338	14.48520557	1.30099678	1.96E-05	0.000766962
SBSN	997.1851328	3405.118323	1.771771652	1.99E-05	0.000774558
AKNAD1	12.18708606	93.63322946	2.9416674	2.03E-05	0.000787849
HIST1H4E	28.78106351	85.53008937	1.571312144	2.17E-05	0.000830225
MRO	20.06799259	42.52354694	1.083365628	2.21E-05	0.000842043
ST13P20	1.505262075	4.622069809	1.618524359	2.35E-05	0.000893066
DSC1	17.4766609	137.7091523	2.978122972	2.37E-05	0.000896102
EPYC	33.64069978	126.9326615	1.91578372	2.48E-05	0.000925471
TRBV2	9.672407333	3.968028788	-1.285452509	2.50E-05	0.000934999
TRGV2	3.250945248	1.120575735	-1.536619101	2.57E-05	0.000956345
KIF26A	113.3283531	255.6895444	1.17388432	2.69E-05	0.000985387
AIM2	1543.016101	704.2705454	-1.131551465	2.78E-05	0.001012067
HTR4	1.878943838	0.911751819	-1.043208867	3.05E-05	0.001089935
TCHHL1	6.966676701	27.71013364	1.991871149	3.09E-05	0.001097046
TRAV8-3	8.72264061	3.98683791	-1.129519997	3.24E-05	0.001130352
TRAC	1218.051787	589.5551493	-1.046876792	3.40E-05	0.001175966
TRAV6	3.412985112	1.35988871	-1.327545531	3.42E-05	0.001178608
TRAV16	4.631913457	2.082791179	-1.153090096	3.74E-05	0.001254869
SPSB4	22.99662376	65.35915201	1.506967198	4.04E-05	0.001332969
AC090617.1	0.561770054	1.142048456	1.023572239	4.08E-05	0.001337338
SLC22A2	2.8739344	13.599672	2.24247282	4.08E-05	0.001337338
PAEP	34.62285357	90.68656002	1.389164121	4.22E-05	0.001374915
CTSV	664.2910466	1467.483922	1.143457322	4.35E-05	0.001403612
CORO6	182.9047345	400.2703348	1.129882278	4.56E-05	0.001461725
RP11-417L19.2	1.59996189	4.52316787	1.499295999	4.71E-05	0.001490885
RP11-277P12.9	21.45676247	10.40278127	-1.044463114	4.69E-05	0.001490885
RP1-122P22.4	36.44588195	104.9710025	1.526163131	4.74E-05	0.001497073
LCE3D	11.5864787	208.0826339	4.166642484	4.92E-05	0.001541128
EOMES	82.1642204	31.7493369	-1.371783827	4.99E-05	0.001557603
ENPP1	150.7744405	661.7018501	2.133789432	5.19E-05	0.001610301
MMP3	659.2607558	1566.998977	1.249083129	5.26E-05	0.001626591
C6orf15	31.87627561	291.6909981	3.193885883	5.54E-05	0.001693428
AC008063.3	0.711298582	1.896219393	1.414598701	5.57E-05	0.001694138
SIT1	171.7007243	65.4306305	-1.391858048	5.57E-05	0.001694138
GPR18	53.53166594	22.05164635	-1.279506181	5.60E-05	0.001698141
RP11-674P19.2	1.448388364	4.056113424	1.485649504	5.69E-05	0.001716544
TRBV10-2	3.383581075	1.201088042	-1.494209051	5.79E-05	0.001743659
PDGFRL	210.383586	425.543973	1.016286068	5.84E-05	0.001753309
BIRC7	17.42172671	44.66632472	1.358299931	5.99E-05	0.001790741

LGALS17A	101.1170776	19.18534511	-2.397950052	6.27E-05	0.001856471
TRBV5-1	23.75472421	10.97099231	-1.114520435	6.45E-05	0.001903849
RP11-367F23.2	3.900880136	15.42787784	1.983668054	6.59E-05	0.001933848
P2RY10	61.12231251	29.66312011	-1.043028772	6.98E-05	0.002018523
TBC1D10C	523.2817781	248.9296428	-1.071849983	7.05E-05	0.002028308
CDSN	14.47231349	42.17562288	1.543113811	7.05E-05	0.002028308
TRBV12-4	6.761127043	3.351418695	-1.012491821	7.11E-05	0.002033538
LINC00520	18.69536518	78.54116741	2.07076839	7.11E-05	0.002033538
AC112721.2	10.29351199	23.12347161	1.16762272	7.22E-05	0.00205073
SHOX2	86.84666222	177.1875744	1.028735128	7.42E-05	0.002098451
TRBV9	14.3690393	5.317411604	-1.434167557	7.56E-05	0.002126419
RP11-95H3.1	1.391269538	3.562347448	1.356426286	7.59E-05	0.002129355
TRAV12-3	8.98712989	4.20004254	-1.097456513	7.77E-05	0.002169587
RP11-68I3.10	2.063230728	4.158766586	1.01125055	7.79E-05	0.002169587
CACNG8	13.32859672	33.14548598	1.314287509	7.95E-05	0.002192737
RP11-44K6.2	9.246919496	3.593833979	-1.363449065	8.24E-05	0.00225912
AC006369.2	3.956528571	1.916675463	-1.045629099	8.28E-05	0.002266173
TRBV3-1	8.903515719	3.574018662	-1.316827956	8.62E-05	0.002336459
AC008063.2	1.113151664	2.413443544	1.11644291	8.70E-05	0.002353502
PLXNA4	63.64669673	130.5850305	1.036831979	9.05E-05	0.002415387
MYH2	2.631543586	5.61600736	1.093635536	9.25E-05	0.00245705
TRAV8-6	12.40408705	5.246112485	-1.241494909	9.46E-05	0.002504611
FGF5	27.68015472	65.66036247	1.246170707	9.52E-05	0.002514615
TRAV10	2.422858961	0.939698982	-1.366439834	0.00010026	0.002613229
AC012668.2	2.032365161	11.30783775	2.476091544	0.000100472	0.002616021
TRAV5	4.362500403	1.942410191	-1.167307369	0.000103063	0.002666851
KLK8	184.1037383	368.485504	1.001088944	0.000108228	0.002776458
CYP4F35P	182.7523488	84.20376791	-1.117933251	0.00011017	0.002812991
LINC00158	5.941093908	1.565424888	-1.924174306	0.000114196	0.002886357
TRBV4-2	12.56326385	6.217671198	-1.014765084	0.000117105	0.002947988
TRBV29-1	19.23293861	7.564565065	-1.346250169	0.000120364	0.00302644
DCSTAMP	9.918295788	42.59344218	2.10246717	0.000125085	0.003102098
PCAT29	5.59682003	2.117410915	-1.402306085	0.000126273	0.003124708
RP11-116D17.1	6.27374809	2.440028835	-1.362429405	0.000127966	0.003151707
KIR3DL2	6.015523039	0.959540537	-2.648274521	0.000130696	0.003207815
SLC19A3	52.64467706	109.6352406	1.058352034	0.000134367	0.003258109
LYVE1	134.4202252	437.9460118	1.704002806	0.000134825	0.003262906
TRAV4	10.86675901	4.564579281	-1.251367926	0.000140512	0.003367981
LY6G6C	86.84337249	255.5859203	1.557320705	0.000142111	0.003396568
LAMP5	112.4389855	232.6199911	1.048832744	0.000146268	0.003479317
RP11-1028N23.3	3.248270947	1.617813862	-1.005626349	0.000147419	0.003503368
CXCL13	1964.486915	588.5564423	-1.738899877	0.000150281	0.003554526
CXCL9	4671.5155	1543.678235	-1.597518587	0.000151813	0.003573875
KIAA1644	107.4828041	217.8629191	1.019314802	0.000151813	0.003573875
RP11-184A2.2	1.407964748	2.881506964	1.033212294	0.000153351	0.003606693
RP11-567M16.2	0.946661735	2.232590986	1.237798058	0.000154505	0.003627027
RP11-143006.1	1.167877801	2.515265076	1.106821121	0.000155997	0.003655208
ENDOU	14.09227987	73.51786711	2.38318988	0.000157021	0.003668895
TRAV24	3.366264074	1.148828725	-1.550984629	0.000159522	0.003710566

HLA-DOA	1821.685971	887.9223997	-1.036768781	0.000163501	0.003781503
IL36B	3.357261375	13.23653397	1.979168631	0.000163439	0.003781503
GFY	8.60057541	42.95930015	2.320465401	0.000166154	0.00381818
PSG9	4.357768983	16.36122544	1.908619186	0.000174192	0.003966499
CD7	691.0386481	339.7161007	-1.024436804	0.000186328	0.004163367
CD27	256.1009439	122.5068631	-1.063849996	0.00019588	0.004307633
CARMN	61.43887299	140.1257041	1.189497965	0.000203175	0.004440773
TRGV3	3.711261222	1.770174446	-1.06801801	0.000210179	0.004547844
RAET1L	49.00502254	105.2716989	1.103116113	0.000213849	0.004586043
TRBV7-9	25.99499755	10.57579228	-1.297468274	0.00021526	0.004608398
RP11-120C12.3	1.281344266	6.204436679	2.275642084	0.000217614	0.004638983
KIR2DS4	23.8053517	2.479341756	-3.26325689	0.000221681	0.004693707
TRBV5-5	2.701692203	1.248585026	-1.113569253	0.000228932	0.00481282
C4orf26	51.31294193	103.9777453	1.018880129	0.000243238	0.005026918
CD36	1632.563063	4839.477039	1.567712435	0.000255922	0.005211645
RP1-140J1.1	0.912527659	1.98689949	1.1225787	0.000258341	0.005243854
TRBV21-1	2.072681097	0.751614375	-1.463433596	0.000265179	0.005324609
RP11-310H4.6	1.039940703	2.315163312	1.154612696	0.00026654	0.005338114
RP11-757O6.1	14.49081726	7.011891293	-1.047263428	0.000295298	0.005713328
CARD18	7.395122031	23.02943591	1.638833215	0.000304695	0.005852754
GNLY	928.1712097	401.270675	-1.209815221	0.000305114	0.005856316
TRBV15	4.482392759	1.697475772	-1.400878084	0.000308011	0.005902875
HSPB3	9.357601456	27.43695984	1.551909942	0.000326153	0.006151726
GRM6	18.85661823	47.358507	1.328552635	0.000335823	0.006300897
RP4-529N6.2	0.927127263	5.641186397	2.605159317	0.000336519	0.006301732
CLCA4	3566.497237	1474.369802	-1.274409429	0.000352686	0.006501294
CP	3607.845761	1429.411705	-1.335716156	0.000367733	0.006718436
RPE65	12.65812639	37.89348591	1.581885985	0.000368413	0.006725952
WNT9B	4.419997127	12.4077649	1.489125919	0.000368733	0.006726885
SLAMF6	215.3855831	98.39956817	-1.130197796	0.000379675	0.006861543
ANXA10	2421.00856	994.9097359	-1.282970634	0.000389952	0.007001803
LPA	39.90593805	16.45618263	-1.277973727	0.000397676	0.007074567
AC002331.1	27.88583766	11.61013491	-1.264147872	0.000408752	0.007184394
BTLA	47.19239748	23.37645027	-1.013498593	0.00040853	0.007184394
LY6H	23.06199427	78.96128411	1.775628177	0.000412306	0.007214279
RP11-342M1.7	3.283776645	16.57676574	2.335734646	0.000440162	0.007598336
KRTDAP	683.8469756	2471.009744	1.853355265	0.000440567	0.007600079
ZFP42	37.08675272	109.5258052	1.562294964	0.000446015	0.0076782
FCMR	453.7470206	219.576214	-1.04716639	0.000446423	0.007679954
NLRP12	9.725478156	30.24016026	1.636624698	0.000449252	0.007712717
SP140	312.1590989	154.8006912	-1.011869605	0.000452097	0.007735059
SPRR2E	233.596556	1243.334793	2.412123915	0.000478263	0.008072469
TRAV22	4.131320825	1.80346945	-1.195828115	0.000521667	0.008591059
DSC2	2937.19047	6126.92854	1.060727201	0.000527284	0.008643585
HMGB3P32	2.173554079	1.028305874	-1.079786527	0.000542871	0.008818311
RP11-540O11.6	0.947375225	2.28619306	1.270939389	0.000555604	0.008972767
SPRR2G	58.43423975	455.8707732	2.963739044	0.000568519	0.009140085
LINC00545	0.925955255	2.759701328	1.575497753	0.000571949	0.009189331
KCNH2	171.2781747	501.0451172	1.548599193	0.000582509	0.009317175

LINC00922	5.761701381	12.18430044	1.080456626	0.000588379	0.00939306
PTGIS	1100.069098	2218.107407	1.01173508	0.000597134	0.009508583
CTA-833B7.2	6.485190229	28.20966166	2.120968564	0.000606441	0.009626227
RP11-212I21.3	0.928298565	1.901057599	1.03414145	0.000612765	0.009696734
TRBV19	19.64383288	9.816804867	-1.00075101	0.000613208	0.009696734
RP11-442J21.2	2.61896279	6.213801951	1.246480698	0.000639403	0.009947683
ZNF114	139.4101978	286.4906789	1.039152103	0.000639131	0.009947683
PRR9	203.2423296	565.4947968	1.476312844	0.000638102	0.009947683
RP11-119J18.1	2.830513339	6.882012243	1.281766736	0.000653488	0.010091593
FCRL6	39.58793965	16.92524238	-1.225884491	0.000654062	0.010093062
RP11-47I22.2	14.9604218	31.36709128	1.0681009	0.000680709	0.010396592
SPRR2B	12.47249762	88.73448892	2.83074456	0.00069458	0.01055694
ZNF80	7.17909911	3.458135993	-1.05380821	0.0007024	0.010633103
RHOT1P1	8.68776887	4.101473812	-1.082843305	0.000707859	0.010681
AC092484.1	1.688734866	62.6706819	5.213775945	0.000712225	0.010733936
DDN	29.13517753	60.22536865	1.047609218	0.000713825	0.010745129
LAG3	649.5064997	295.5605741	-1.135890127	0.000720403	0.010824621
SLAMF1	178.6017863	78.25901341	-1.190417682	0.000724819	0.010851917
RP11-275N1.1	1.071708998	3.543322923	1.72518973	0.000731737	0.010935888
RNF222	18.6249587	38.25888824	1.038557725	0.000733718	0.010958962
C1orf105	4.524619812	16.59229471	1.874644947	0.000750265	0.011113327
AC002066.1	5.306503114	11.61774191	1.130496315	0.000757879	0.011212856
KRT79	129.8869281	537.7771092	2.049752103	0.000760834	0.011246675
SRD5A2	101.6638177	24.78122483	-2.036486912	0.000765523	0.011295356
CTC-518B2.8	30.62771953	71.45199893	1.222136421	0.000773708	0.011373147
LCE3E	5.115957563	79.48351593	3.957579489	0.000798091	0.011635958
HNF4G	174.7380872	86.8145808	-1.00918483	0.000816069	0.011836823
KLK15	1.005798652	3.008282416	1.580598488	0.000838079	0.012031271
OLAH	3.096841798	6.390124137	1.045046273	0.00085986	0.012237367
TRBV18	10.02300956	4.944464246	-1.019429652	0.000863119	0.012262845
RP11-308D13.3	2.420829015	5.176782559	1.096554537	0.000895155	0.012596541
RP11-354E11.2	6.246952458	36.01274878	2.527283266	0.000896156	0.012596896
TRBV5-6	8.085603678	3.453677702	-1.227222034	0.000899645	0.012631343
GZMK	169.2436819	72.29387525	-1.227156645	0.000933274	0.012951055
AC105053.3	4.101415863	1.988839271	-1.044195345	0.000945166	0.013043808
TRAV2	6.934333222	3.385151457	-1.034536782	0.000974125	0.013312052
TRBV11-2	7.057594564	2.992200284	-1.237969809	0.00097658	0.013330449
LINC00704	41.6973845	97.79318865	1.229777092	0.000991748	0.013464128
CLDN6	84.63886422	281.1463746	1.73192927	0.00099439	0.013492674
RP11-150O12.6	30.70685697	71.44697264	1.218312031	0.001028486	0.013813177
ZNF676	24.87675365	51.21582216	1.041791343	0.001139001	0.014905801
TRDC	92.02575988	42.26015325	-1.122739758	0.001152877	0.015032417
NOG	35.42680266	117.3999919	1.728519139	0.001181474	0.015278912
RP11-69L16.6	6.67520169	13.63419859	1.030346569	0.001211299	0.015559287
PEG3	123.2639157	270.619313	1.134514275	0.001221055	0.015652496
FRMPD2B	2.510211227	1.187978735	-1.079299756	0.001225393	0.01569205
AC073850.6	3.080052322	9.802004109	1.670121893	0.001239694	0.015842789
RP11-465L10.10	9.541078558	23.1537282	1.279020246	0.001268325	0.016104707
NPW	17.97615277	36.86565292	1.036193018	0.001268548	0.016104707
HMP19	15.21781022	43.97553521	1.53094036	0.001289279	0.016285353

FMN2	19.883854	45.47348058	1.193428018	0.001291336	0.016303113
RP5-1171I10.5	106.287454	52.2486402	-1.024505917	0.001317755	0.016569837
PPBP	13.1307287	85.29051199	2.699438278	0.001338441	0.016796222
PCSK1	68.53268464	142.0974678	1.052016737	0.001344971	0.016835994
RPS20P22	2.314133324	7.579761016	1.711680378	0.001355011	0.016936281
TOMM20P2	6.130765179	2.928243463	-1.066031639	0.001356748	0.016949532
RP11-973F15.2	0.385718511	2.30688974	2.580328763	0.00136491	0.017026025
CTD-2288O8.1	5.551808074	2.132042771	-1.380721314	0.001415892	0.017479189
MIR155HG	81.85243752	40.21016698	-1.025465053	0.001417354	0.017488609
CTB-134H23.2	6.909802412	2.326691754	-1.570364365	0.001420283	0.017513621
SPRR1B	1944.797063	5809.686505	1.578840697	0.001450603	0.017750952
CTSE	4605.786122	1250.641453	-1.880779177	0.001486836	0.018026263
SPRR2D	423.7572013	1403.837709	1.728066372	0.001496527	0.018117449
RP11-25L3.3	2.040473537	6.583449965	1.689939806	0.00161247	0.019132714
PCNPP3	1.945676787	6.738065977	1.792062483	0.001616756	0.019173346
UTS2	92.62123222	11.08536897	-3.06268616	0.001643712	0.019356696
CYP2F1	13.33627426	36.11158958	1.437106248	0.001647193	0.019379474
AC004160.4	0.745342483	1.501960224	1.010871209	0.001722322	0.019926434
NOTUM	189.3616745	3238.294918	4.096018107	0.00181021	0.020647609
CTC-353G13.1	1.282333484	3.15553179	1.299111659	0.001823551	0.020752524
CTD-2194D22.3	4.57340598	12.21587454	1.417416252	0.001828587	0.020781513
AC006262.5	266.6104839	600.2383975	1.170802099	0.001899797	0.021426728
TRBV5-4	8.342910751	3.657683042	-1.189620749	0.00192574	0.021679071
POM121L9P	16.77161141	39.17406946	1.223877696	0.002115332	0.023188114
ANGPTL1	79.82607101	231.157223	1.533942534	0.002133264	0.023343814
CD52	1099.218429	496.8697458	-1.145538492	0.002133264	0.023343814
PGBD4P1	1.650639576	0.663366809	-1.3151464	0.002144594	0.023447307
TRBV12-3	3.809056893	1.751816725	-1.120581989	0.002155438	0.023483866
KRTAP2-3	6.723058469	27.18039687	2.01537692	0.002157332	0.023484641
NEU2	0.258887702	2.962732751	3.516530156	0.002194633	0.023755904
RP11-59N23.1	0.723087139	1.633153213	1.17541872	0.00221222	0.023898447
RP11-662I13.2	2.540184665	5.857478987	1.205346492	0.002219753	0.023945041
CDH16	36.26852336	76.56260353	1.077921881	0.002246861	0.024143874
CGB8	8.00547165	86.92584217	3.440726831	0.002335093	0.024810038
KIR2DL3	7.793481775	1.561256775	-2.319560171	0.002370078	0.024996093
OGN	99.08771016	246.8579764	1.316903225	0.0023859	0.02505839
FCRL3	115.0070575	40.73676673	-1.497319012	0.002392585	0.025106609
RP11-383J24.1	1.000645958	2.329306582	1.21896892	0.002395052	0.025111451
HIST1H2BF	22.68207092	45.62857893	1.008385356	0.002412676	0.025232866
AC011523.2	0.743441797	3.860757689	2.376592306	0.002416576	0.025263103
CILP	580.5942572	1166.184894	1.006194333	0.002419438	0.025282466
AVPR1A	151.6276473	336.5466613	1.15027371	0.002426178	0.025331771
LEP	31.83520848	89.26624605	1.487491545	0.002458664	0.025628224
CBLN4	2.849515263	7.025437653	1.301871581	0.002486793	0.02584406
RP11-542M13.3	4.662615402	0.98261644	-2.246439151	0.002666801	0.027186823
SCN2B	8.272068392	18.86073759	1.189066078	0.002701186	0.027489433
TMEM229A	3.582906082	11.45882979	1.677257588	0.002701972	0.027489433
RP11-761N21.1	1.043339407	2.397920683	1.200575384	0.002762584	0.027884595
AC007250.4	1.927599447	5.697328441	1.563480285	0.002791683	0.028105338

TRAV8-1	4.426329382	2.131368921	-1.05433048	0.002832729	0.028415777
LINC01522	1.016265932	3.897561534	1.939293831	0.002847945	0.028522723
CRTAC1	4425.785122	1190.26624	-1.894649094	0.002887177	0.028754686
AARD	22.22792644	48.1324556	1.114636657	0.00292241	0.029013288
RP3-492J12.2	1.875289743	0.647448849	-1.534275394	0.003058013	0.029850782
LCE2B	0.191290662	4.326903741	4.499496673	0.003089059	0.030083498
IRX4	37.82972266	131.0710761	1.792757252	0.003133265	0.030387988
RP11-445F12.2	0.704477428	1.915395215	1.443016714	0.003226458	0.03099803
RP11-398B16.2	5.891009332	23.24903065	1.980583822	0.003253831	0.031179634
L1TD1	6.116225825	18.90873627	1.628339366	0.003321383	0.031584665
CXCL11	1808.755361	754.5351628	-1.261337253	0.003371758	0.031882144
RP11-71H17.8	2.078571857	4.475639977	1.106501366	0.003436578	0.03228785
RP11-513N24.1	0.981305013	2.516019431	1.358369528	0.003449053	0.032344393
RP11-116O18.3	48.43318159	22.25582843	-1.121812574	0.00346126	0.032434579
RP11-116D17.4	2.887985133	1.052241621	-1.456597294	0.003579197	0.033267686
RTL1	17.08351114	50.39220354	1.560596024	0.003631343	0.033588584
LY9	128.8897286	56.05799679	-1.201145202	0.003714828	0.034121379
PLD5	14.73984894	35.45923556	1.266439696	0.003775534	0.034464132
TRAV25	3.286691783	1.599669559	-1.03886225	0.003810076	0.034653152
FGF16	1.704420869	6.956536802	2.029087642	0.003813222	0.034669182
AC079610.2	8.437912372	3.04400949	-1.470913248	0.00395898	0.035619571
LCE2C	0.417195062	3.211882312	2.944625043	0.004052499	0.03608496
RP11-373E16.3	0.684546569	1.546469428	1.175757718	0.004051292	0.03608496
KRTAP3-1	5.722265365	157.2301377	4.780147565	0.004103958	0.036465396
LINC01395	2.686108093	6.411325547	1.255105304	0.004127538	0.036609979
U82695.9	1.521388524	3.339649244	1.13430796	0.004127538	0.036609979
CLC	5.367112782	18.10187235	1.753920819	0.004150079	0.036744847
LINC01077	0.764144971	2.417480478	1.661585968	0.004193653	0.037012904
CR1L	16.72037572	6.945991608	-1.267354693	0.004322695	0.037863815
LIN28A	1.553110954	98.45988904	5.986303309	0.004407173	0.038376814
IGFL1P1	43.05754558	88.04798816	1.032023956	0.004482406	0.038782488
CTD-2114J12.1	7.172692139	3.163911583	-1.180805426	0.004529984	0.039099599
NF1P6	1.517821867	3.86072484	1.34686925	0.004561137	0.039287261
LINC01510	0.756129471	2.11985729	1.487261954	0.004568143	0.039317632
C1QTNF1-AS1	3.366360698	7.124756054	1.081650852	0.004588318	0.039412956
ACP5	2152.814441	4643.214633	1.108899997	0.004605539	0.039506693
DHRS7C	0.177532799	1.450116454	3.030011271	0.004688725	0.040028355
RP11-93H12.4	0.885250141	1.876585254	1.083952761	0.004701158	0.040107156
LCE3C	0.503624072	1.817340043	1.851409242	0.0047413	0.040298633
RP11-25L3.1	0.609210511	1.512056848	1.311499643	0.004747223	0.040335289
CGB5	15.39770422	268.5527934	4.124418561	0.004877416	0.041104402
RP11-305F18.1	1.314996999	4.547532404	1.790024411	0.004882608	0.041122922
PIWIL3	12.3405963	39.01669467	1.660679457	0.004902416	0.041236634
TCHH	76.57223743	234.8830535	1.61704931	0.004917161	0.041289007
NKD1	231.1153986	879.6477893	1.928312599	0.004930016	0.041369192
RP11-148B18.1	3.206326766	8.916739629	1.475594829	0.00495508	0.041530006
MS4A8	229.1943254	110.4887855	-1.05267138	0.005015691	0.04191768
PCDH11Y	6.895516497	3.072639324	-1.16618019	0.005023033	0.041924999
OPN4	3.031765013	6.279322213	1.050450907	0.005108295	0.042436947

RP11-522B15.6	0.587511216	1.394114847	1.246661115	0.005161806	0.042656852
RP1-300G12.2	0.844391862	2.1861837	1.372430053	0.00530634	0.043435688
LCE1A	0.360463425	3.966414413	3.459910633	0.005322995	0.043529345
FAM25A	52.06841784	176.9762944	1.765075652	0.00538133	0.043863183
RP3-407E4.3	1.242126497	2.806101161	1.175754915	0.005386777	0.043879023
ADAMTS9-AS1	29.61740369	60.88612396	1.039668296	0.005413264	0.044037491
SERPINB7	151.3749665	494.0405715	1.706502883	0.005449564	0.044261026
MARCO	341.8311433	703.27647	1.040808106	0.00545552	0.044272324
BPIFB1	2028.862027	293.3761464	-2.789847278	0.005531628	0.044660993
KLK9	1.004289007	3.120442715	1.635576229	0.005605058	0.045070784
LGALS7B	141.2409348	756.5289006	2.421236923	0.005623943	0.045179125
AC005150.1	0.413566411	13.26616832	5.003488908	0.005631699	0.045226929
RP11-402P6.9	5.762922114	27.6860955	2.264289181	0.005731329	0.045821366
TRAV38-1	2.189598917	0.8948687	-1.290918703	0.005773685	0.046101134
RP11-1020M18.10	1.006254135	5.252858381	2.384107978	0.005824552	0.046315359
RP11-654A16.1	0.263348762	0.816351696	1.632216143	0.005917825	0.04681923
CASC17	0.29718727	2.86188186	3.267519895	0.005924821	0.046830206
LVRN	27.68702864	152.3720592	2.46031624	0.006031223	0.047521259
RP11-138H8.2	0.429168464	1.308478614	1.60827437	0.006117563	0.048005236
KRT34	20.96417173	147.6209691	2.815899929	0.006131594	0.048030762
RP11-221N13.4	1.26504895	2.617678567	1.049094745	0.006220161	0.04855176
RTBDN	18.42611046	42.00493803	1.188807372	0.006266545	0.048764005
KRT15	16696.68033	7230.93562	-1.207307054	0.006314921	0.048940638
LINC00302	0.464946992	2.159647987	2.215658027	0.006319666	0.048948663
COL9A1	120.3313174	44.45877159	-1.436472175	0.006329731	0.048989679
TLL1	105.1001767	211.7067036	1.010301858	0.006379571	0.049152723
RP11-432M8.17	1.104453942	24.67453369	4.481617659	0.006450985	0.049565727

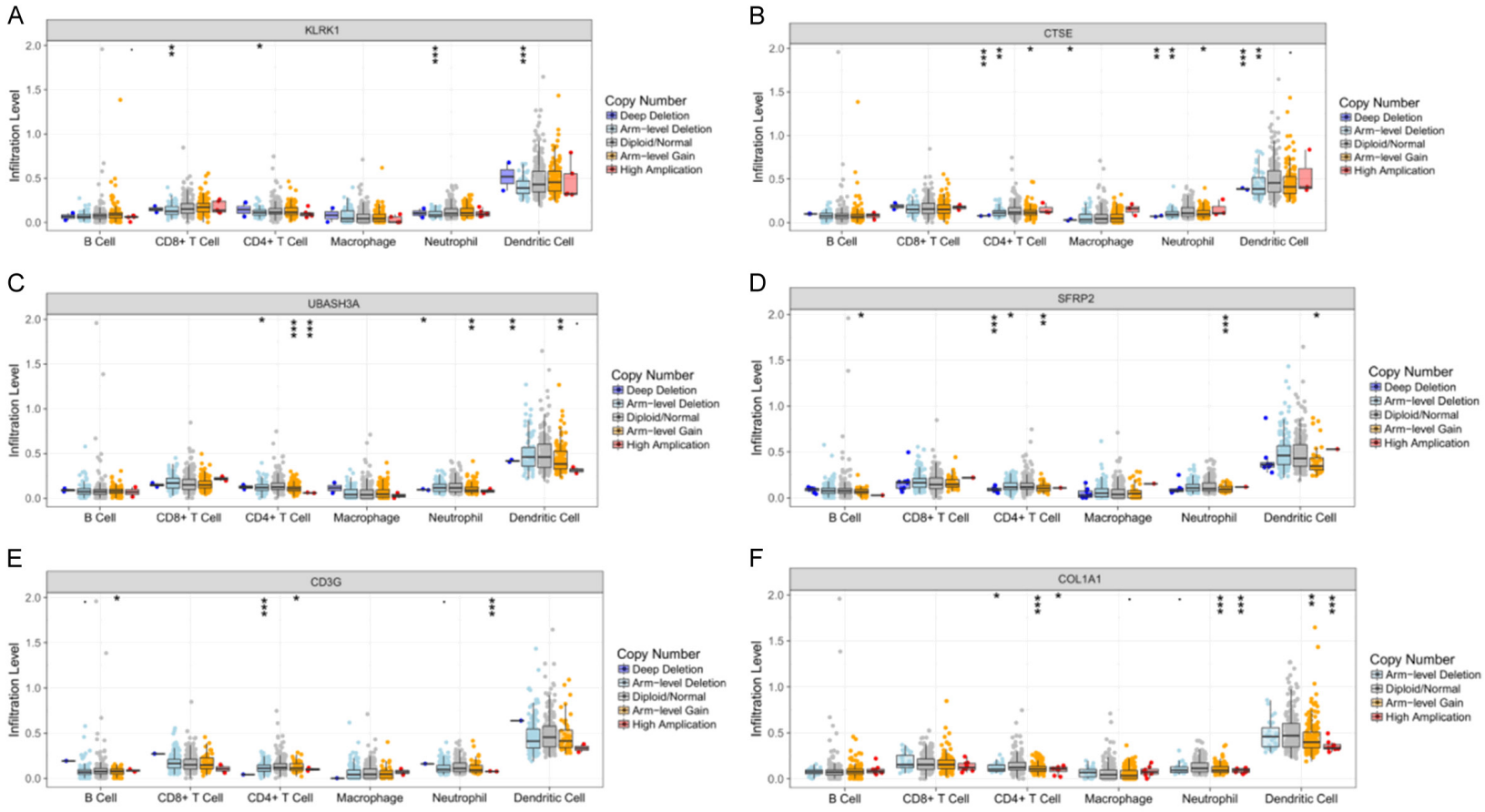

Figure S1. Associations of several hub TIICS-related signature mutants with immune cells infiltration based on "SCNA" module in TIMER database. A-F. Mutants of 6 identified signature conferred the low infiltration levels of immune cells, especially especially $CD4^+$ T cell, neutrophil and dentritic cell.